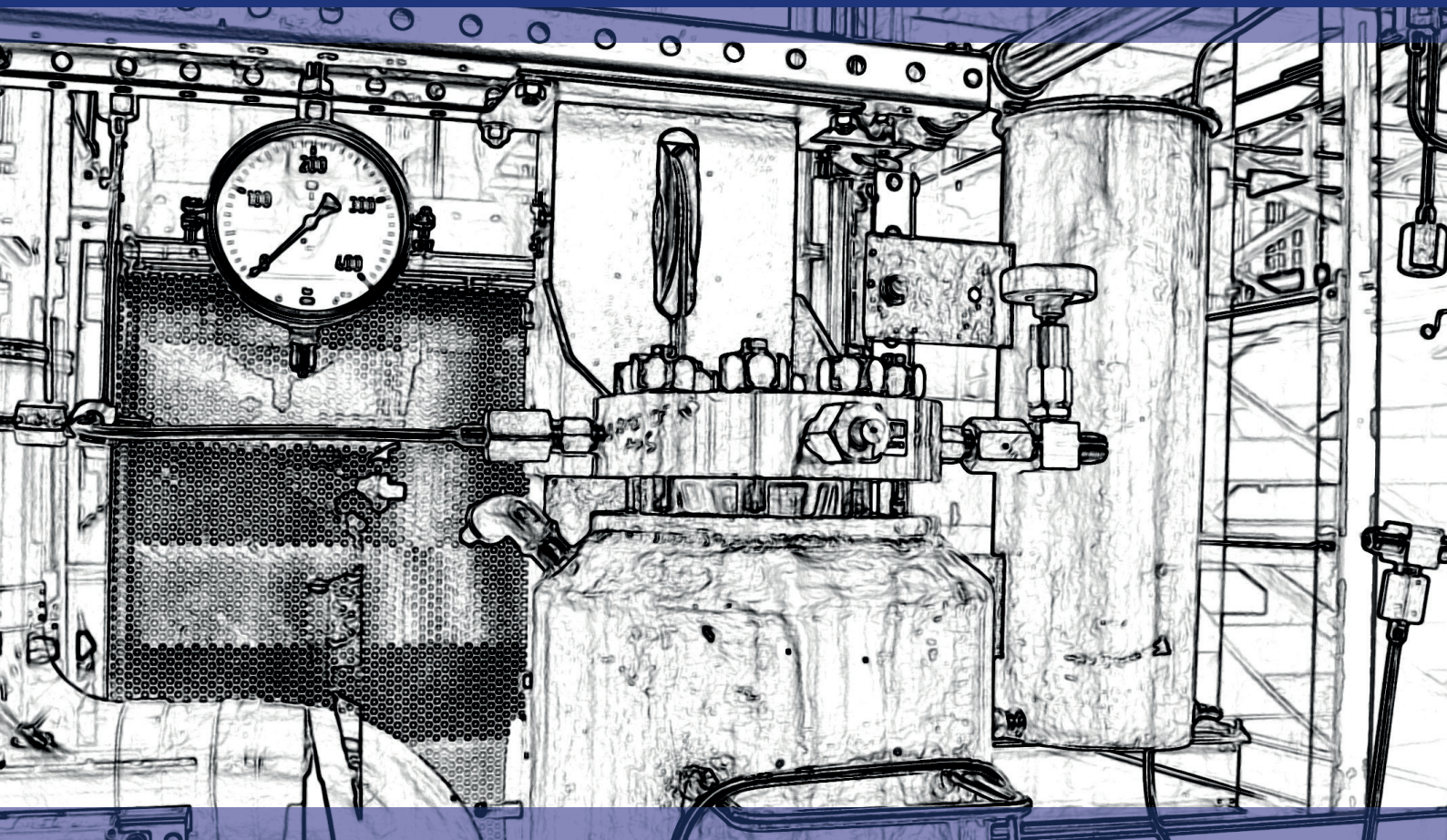


Thomas Gamse (editor)

Book of Abstracts

ESS-HPT 2017



The European Summer School in
High Pressure Technology

02.07. - 16.07.2017

Impressum

Organisation: Thomas Gamse
Institute of Chemical Engineering and Environmental Technology
Central Lab Biobased Products
**Graz University of Technology, Inffeldgasse 25/C, A-8010 Graz,
Austria**
Tel. +43 (0)316 873-7477
Email: Thomas.Gamse@TUGraz.at

Zeljko Knez
Amra Perva-Uzunalić
Faculty of Chemistry and Chemical Engineering
Laboratory for Separation Processes
University of Maribor, Smetanova ulica 17, 2000 Maribor, Slovenia
Email: zeljko.knez@um.si; amra.uzunalic@um.si

Editor: Thomas Gamse
Layout: Thomas Games, Stefan Schleich
Cover: Thomas Games, Stefan Schleich

© 2017 Verlag der Technischen Universität Graz

www.ub.tugraz.at/Verlag



This work is licensed under a Creative Commons Attribution 4.0 International License.

<https://creativecommons.org/licenses/by/4.0/deed.en>

Book of Abstracts, ESS-HPT 2017 The European Summer School in High Pressure
Technology
2.7.-16.7.2017, University of Maribor and Graz University of Technology

ISBN (e-book) 978-3-85125-541-6

DOI 10.3217/978-3-85125-541-6

Year of Publication: 2017

Preface

The European Summer School in High Pressure Technology (ESS-HPT) is the continuation of many years of high pressure intensive courses. The history of this very successful series of courses started in 1995, when the first intensive course took place in Monselice, Italy. Most of these Intensive Courses were supported by SOCRATES and later Life Long Learning, as shown in following overview:

SOCRATES IP "Current Trends in High Pressure Technology and Chemical Engineering"

1995 Monselice / Italy
1996 Nancy / France
1997 Erlangen / Germany

SOCRATES IP "High Pressure Technology in Process and Chemical Engineering"

1999 Abano Terme / Italy
2000 Valladolid / Spain
2001 Maribor / Slovenia and Graz / Austria

SOCRATES IP "High Pressure Chemical Engineering Processes: Basics and Applications"

2002 Graz / Austria and Maribor / Slovenia
2003 Budapest / Hungary
2004 Barcelona / Spain

SOCRATES IP "Basics, Developments, Research and Industrial Applications in High Pressure Chemical Engineering Processes"

2005 Prague / Czech Republic
2006 Lisbon / Portugal
2007 Albi / France

Life Long Learning IP "SCF- GSCE: Supercritical Fluids – Green Solvents in Chemical Engineering"

2008 Thessaloniki / Greece
2009 Istanbul / Turkey
2010 Budapest / Hungary

EFCE Intensive Course "High Pressure Technology - From Basics to Industrial Applications"

2011 Belgrade / Serbia

Life Long Learning IP "PIHPT: Process Intensification by High Pressure Technologies – Actual Strategies for Energy and Resources Conservation"

2012 Maribor / Slovenia and Graz / Austria
2013 Darmstadt / Germany
2014 Glasgow / Great Britain

Unfortunately the financial support for these Intensive Programmes was cancelled within ERASMUS+. The EFCE Working Party "High Pressure Technology" decided in September 2014 to go on with this course in the form of a Summer School.

ESS-HPT "The European Summer School in High Pressure Technology"

ESS-HPT 2015	Maribor / Slovenia and Graz / Austria
ESS-HPT 2016	Maribor / Slovenia and Graz / Austria
ESS-HPT 2017	Maribor / Slovenia and Graz / Austria

The ESS-HPT will take place every year within the first 2 weeks of July at University of Maribor, Slovenia and Graz University of Technology, Austria.

All participants have to give an oral presentation and the abstracts of these presentations, which are peer-reviewed by the EFCE WP Members, are published in this book of abstracts.

The editor

Thomas Gamse
Organiser of ESS-HPT 2017

Many thanks to our sponsors, NATEX Prozesstechnologie GesmbH and Tourismusverband Stadt Graz,



Contents

Abstracts of Participants Presentations

Monday, 3 July 2017		
16:00 - 16:15	Diana Keddi Polylactide as encapsulation or carrier material for cosmetic applications	1
16:15 - 16:30	Marc Conrad Analysis of the mechanical behaviour of a wheat straw fixed bed in a Liquid Hot Water (LHW) leaching process	4
16:30 - 16:45	Karen Fuchs Development of a CO ₂ -intensified decontamination technology to ensure food safety of low water activity food products	8
16:55 - 17:10	Arian Shoshi Designing a hydrogen compressor for pressure up to 1000 bar with inner cooled walls	9
17:10 - 17:25	Gregor Hostnik , Maša Knez Hrnčič, Martin Gladović, Urban Bren Redox properties of tannins	13
17:25 - 17:40	Paul Peikert , Markus Busch Modelling of high-pressure ethene homo- and co-polymerization	17

Tuesday, 4 July 2017		
16:00 - 16:15	María Andérez-Fernández , Eduardo Pérez, Ángel Martín, Dolores Bermejo Influence of reaction time in CO ₂ hydrothermal reduction	20
16:15 - 16:30	Ana Roda , Vanessa Gonçalves, Isabel Nogueira, Ana Matias, Miguel Moreno, Subbu Venkatraman Encapsulation of ovalbumin in PLGA particles through supercritical fluid extraction of emulsions	24
16:30 - 16:45	Margarethe Roskosz Crystallization of high porous metal-organic coordination complexes by the gas antisolvent method	28
16:55 - 17:10	Tijana Adamović Lignin valorization by hydrolysis in supercritical water	32
17:10 - 17:25	Daniel Steger Inline-pulsation-damper for reduction of pressure pulsation in a Triplex diaphragm pump	36
17:25 - 17:40	Miaotian Sun , Pavel Gurikov, Irina Smirnova, Monika Johannsen Synthesis of stationary phases for chiral separations and thermodynamic studies of adsorption by supercritical fluid chromatography	40

Wednesday, 5 July 2017		
14:55 - 15:10	Judith Janowski Biopolymer foam extrusion – Modelling CO ₂ dispersion and dissolution phenomena in high viscous polymer melts	44
15:10 - 15:25	Marta Ramos Andrés Downstream processing of liquid effluents of biomass hydrothermal processing plants	48
15:25 - 15:40	Ömer Faruk Delibalta Application of fast measurement techniques to safety assessments of the high-pressure LDPE process: decomposition and pressure release	52
16:00 - 16:15	Samuel Theißl , Thomas Gamse Extraction of oil and OPC from grape seeds using supercritical CO ₂ and liquid-liquid-extraction	57
16:15 - 16:30	Robert Kuska Foaming virtualization and characterization of polymeric foams	60
16:30 - 16:45	S. Ehsan Emamjomeh Numerical investigations in a novel low-shear pressure retention valve for hydraulic applications	64
16:55 - 17:10	Sheila Ruiz Barbero Thermodynamic studies of adsorption on porous solids by supercritical fluid chromatography (SFC)	68
17:10 - 17:25	Nikolas Roß Characterization of macromolecular materials under high pressure	72
17:25 - 17:40	Oliver Salman , Markus Busch Parallelization of a Monte-Carlo Model for the simulation of the molecular topology of LDPE	76
17:40 - 17:55	Niklas Strauch Development of novel nozzle geometries for carbon dioxide jet cutting applications	79

Registered Lecturers 82

Registered Participants 84



where innovation... meets experience
 Dense gas technology (CO₂)



YOUR PARTNER FOR SCALE-UP

...we realize your ideas

SUPERCRITICAL FLUID EXTRACTION

NATEX has supplied standard and customized SCF extraction plants to many parts of the world. In some cases applications were implemented on a large scale for the first time. In this way NATEX has established itself as a partner for key industrial projects worldwide.

<p>SPAIN</p> <p>Cork purification plant</p> <p>CORK</p>	<p>ITALY</p> <p>Coffee decaffeination plant Supplied under licenze/Biochemie</p> <p>COFFEE</p>	<p>GERMANY</p> <p>Tea decaffeination plant Supplied under licenze/Biochemie</p> <p>TEA</p>	<p>DENMARK</p> <p>Wood impregnation plant</p> <p>WOOD</p>	<p>INDIA</p> <p>Extraction plant for herbs and spices</p> <p>CHILI</p>	<p>SOUTH KOREA</p> <p>Sesame oil extraction plant</p> <p>SESAME</p>	<p>TAIWAN</p> <p>Rice treatment plant</p> <p>RICE</p>	<p>NEW ZEALAND</p> <p>Extraction plant for hops and nutraceuticals</p> <p>HOPS</p>
--	--	--	--	---	--	--	---

POWDER TECHNOLOGY

Multifunctional high pressure spraying unit, Germany

- PGSS™ and CPF™ process
- Processing range: up to 350 bar, 200°C, 1-50000 mPas
- CO₂ mass flow up to 320 kg/h
- Melt/liquid-mass flow up to 160 l/h
- Explosion proof design (dust and gas)
- Sanitary design (CIP and SIP)



NATEX Prozesstechnologie GesmbH
 Werkstrasse 7
 2630 Ternitz,
 AUSTRIA

www.natex.at

Poly lactide as encapsulation or carrier material for cosmetic applications

Diana Keddi

Institute of Thermo and Fluid Dynamics, Ruhr-University Bochum, Germany

keddi@vvp.rub.de

Introduction

Biodegradable and bio-based polymers provide a sustainable and suitable alternative to petroleum-based materials. Polylactide (PLA) is a common used biopolymer derived from renewable plant sources, such as starch and sugar. Due to its biodegradability, PLA offers various applications in the field of packaging, controlled drug delivery and tissue engineering [1].

Non-biodegradable particles in cosmetic products, so called microplastics, are still a controversial issue, due to their accumulation potential in the environment. In order to avoid this, the substitution of these particles with a biodegradable polymeric material such as PLA may be a solution. The main advantage of using a biodegradable polymer instead of a synthetic non-biodegradable polymer lies in its biocompatibility in the human body and that it can be easily degraded by metabolic pathways [2]. By using the biopolymer as a carrier, active substances can be dispensed. Additionally, the encapsulation enables a controlled release of the contained substances. With focus on cosmetic applications, it is of great interest to encapsulate the active substance urea, a moisturizing agent, with the biopolymer PLA to stabilize and achieve a long term release of the active ingredient.

Experimental

To create a PLA-urea-compound, it is important to understand how the ingredient urea interacts with the polymeric material at high temperatures and pressures. Therefore, the behavior of the system PLA-urea is investigated in a view cell.

For the entire experiments, the PLA resin Ingeo 2003D from NatureWorks LLC and the urea powder ≥ 99.5 % from Carl Roth GmbH + Co. KG are used. In Tab. 1, the material parameters of the PLA resin and the urea powder are specified.

Tab. 1: Material parameters of 2003D PLA and urea $\geq 99.5\%$

Property	PLA	Urea
Density	1.24 g/cm ³	1.32 g/cm ³
M _w	210 000 g/mol	60.06 g/mol
Solubility	-	1080 g/l H ₂ O
MFR (210°C, 2.16 kg)	6 g/10 min	-
D-lactide content	4.25 %	-

Once the behavior of the system PLA-urea is investigated, the enrichment of urea on the surface of PLA particles is studied by using fluidized bed technology. During the coating process, an aqueous urea solution is sprayed with a nozzle on solid fluidized PLA particles. Due to the heated air stream, which fluidizes the particles, the liquid evaporates and a thin urea film dries on the PLA surface. Advantages of coated particles are enhancing storage stability and capability to dose the active agent.

The coated particles serve on the one hand as a low concentrated urea carrier, which can be analyzed on release behavior in further steps. On the other hand, the coated particles can be directly reused in further processing steps to produce highly concentrated PLA-urea-compounds.

The PLA-urea-compounds are to be produced by using a single-screw extruder, shown in Fig. 1.

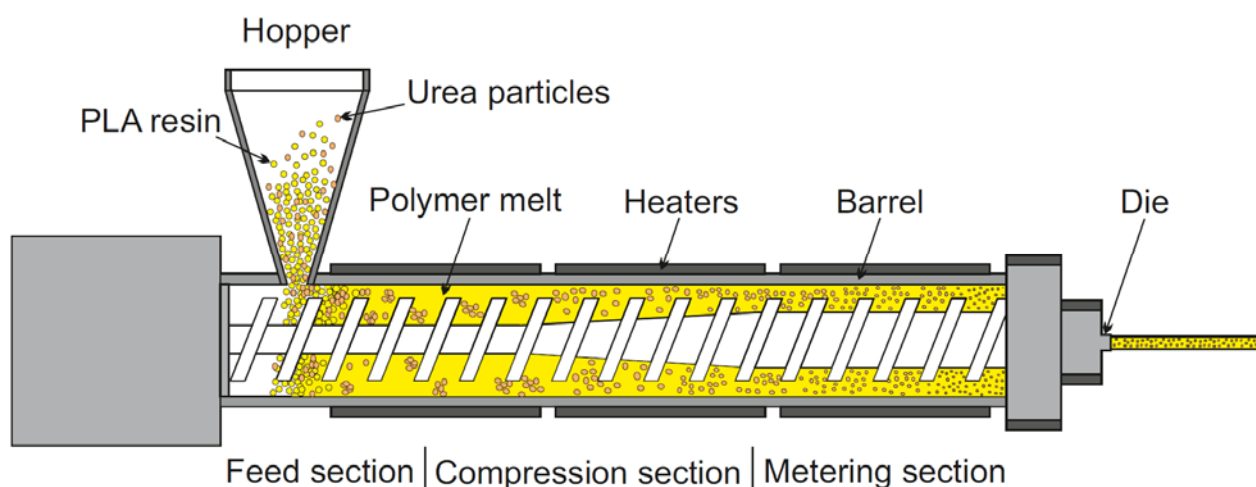


Fig. 1: Single-screw extruder filled with PLA and urea

PLA and (pretreated) urea are added to the hopper and pass different sections while heating and mixing up. The feed section conveys the material along the screw into the compression section, where the decreasing flight depth enhances the friction of the material with the barrel. Finally, the L/D ratio in the metering section determines the shear stress and residence time of the melt [3]. The target is to receive well dispersed urea particles in the polymeric material.

To evaluate the long time release of the active agent urea, the produced samples are investigated with a flow cell and a high performance liquid chromatography (HPLC) plant.

Summary

This work is going to use different technologies for using the biopolymer PLA as carrier or encapsulation material for the active agent urea. The technologies and process parameters are compared with each other and the effect regarding the controlled release of urea is evaluated.

References

- [1] K. Madhavan Nampoothiri, N.R. Nair, R.P. John, An overview of the recent developments in polylactide (PLA) research, *Bioresource technology* 101 (2010) 8493–8501.
- [2] A. Ammala, Biodegradable polymers as encapsulation materials for cosmetics and personal care markets, *International journal of cosmetic science* 35 (2013) 113–124.
- [3] L.-T. Lim, R. Auras, M. Rubino, Processing technologies for poly(lactic acid), *Progress in Polymer Science* 33 (2008) 820–852.

Analysis of the Mechanical Behavior of a Wheat Straw Fixed Bed in a Liquid Hot Water (LHW) Leaching Process

Marc Conrad

Institute of Thermal Separation Processes, Hamburg University of Technology (TUHH)
marc.conrad@tuhh.de

Introduction

The conventional synthesis of pharmaceuticals, polymers, cosmetics and building materials requires carbon from fossil feed stocks. To change the carbon source, new and sustainable processes have to be developed. In the so-called biorefinery of the 2nd Generation, non-edible lignocellulose biomass is fractionated into platform chemicals, which can be used for the above mentioned variety of products. At TUHH- Institute of Thermal Separation Processes (TVT) a two-step process has been developed. First the hemicellulose is leached; in a second step lignin and cellulose are separated by an enzymatic hydrolysis. For experimental work on hemicellulose hydrolysis, a 3 L and a 40 L high pressure fixed bed reactor are in operation, several reference materials (wheat straw pellets, bagasse...) are under investigation.

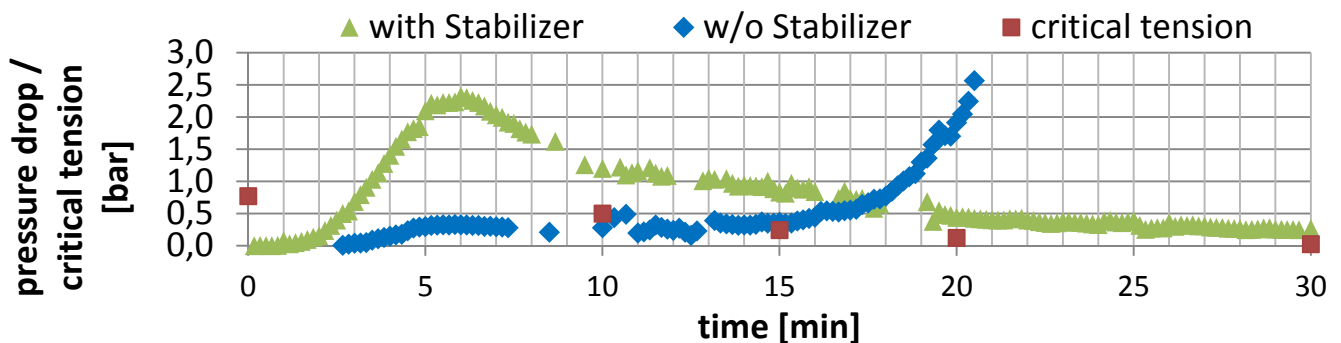


Fig.1: Pressure drop against run time of the LHW for the use of a stabilizer and without; critical tension of the straw bed for corresponding conditions [1]

The Liquid-Hot-Water (LHW) process allows a water throughput at 200°C and 50 bar, with a residence time of about 30 min through the pellet bed. Hereby, it has been observed that the wheat straw bed can be compressed by the fluid flow. Compression of the bed increases the pressure drop. Increasing pressure drop will then compress the bed further. This self-intensifying phenomenon occurs after a certain run time and leads to a shutdown of the plant (see Fig.1). Unfortunately, these mechanically instable conditions are found to be optimal from a kinetic point of view. Installing a perforated

plate in flow direction into the reactor enhances the mechanical stability of the bed. For a Scale-Up of the plant, the mechanical behavior of the pellet bed must be understood. In Fig.1 the pressure drop of a run with and one without stabilizer is plotted against the run time.

Experimental

In a material testing machine the wheat straw from the reactor at defined reaction times were compressed by a piston in the same cartridge used in the very process to a certain bed volume to measure the force inside the straw bed. In Fig. 2 the experimental data gained with the material testing machine is displayed. The composition of the sample has no influence on the tension which the bed can hold. The stronger the bed is compressed, the more tension can be taken up. The corresponding correlation can be seen in equation (1).

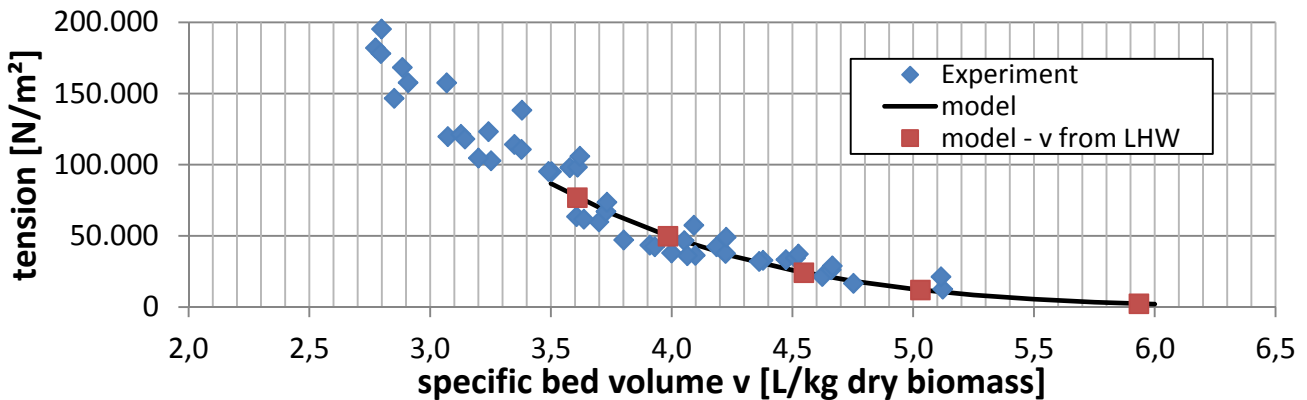


Fig. 2: Bed tension against specific bed volume; Experimental data, model fit, bed volumes from the LHW process marked at the model curve

This curve is interpreted as the critical tension the bed can take up before it is compressed. From mass balances and the reactor geometry the specific bed volume in the reactor is known for the analyzed reaction times. Therefore, the critical bed tension is known for each time step. In Fig.1 the pressure drop and the critical bed tension is plotted against the run time of the reactor. It can be seen that for a run without the use of a stabilizer the bed compresses after the critical bed tension is exceeded.

$$\sigma_{cr} = 10 \cdot \left(8,61 - v \left[\frac{L}{kg_{dry\ bm}} \right] \right)^{5,56} \quad [N/m^2] \quad (1)$$

Modelling

For a more detailed analysis of the stability of the straw bed inside the reactor a bed tension model was derived (eq. (2)), which accounts for the pressure drop of the fluid flow (first two terms), the wall friction (third term) and gravity (last term). The pressure drop was modelled by using a modified Forchheimer equation (eq. (3)). The parameters $k_1(\varepsilon)$ and $k_2(\varepsilon)$ depend on the mean porosity of the bed ε and the correlation fit the process. The friction is obtained from a silo approach, and depends on the Radius R and on the product of the wall friction coefficient λ and the stress ratio K, see [2]. Since both values are unknown an estimate of $\lambda K = 0,2$ was made from literature values. For the viscosity of the fluid the viscosity of water at reactor conditions multiplied by the fitting parameter 3,44, which is a correction for the solubilized sugars.

$$\frac{d\sigma_s(z, t)}{dz} = \frac{\eta}{k_1(\varepsilon)} \cdot u + \frac{\rho}{k_2(\varepsilon)} \cdot u^2 - \frac{2\lambda K}{R} \cdot \sigma_s(z) - (1 - \varepsilon) \cdot (\rho_s - \rho_f) \cdot g \quad (2)$$

$$k_i = \frac{A_i}{(1 - \varepsilon)^{B_i}} - A_i \quad (3)$$

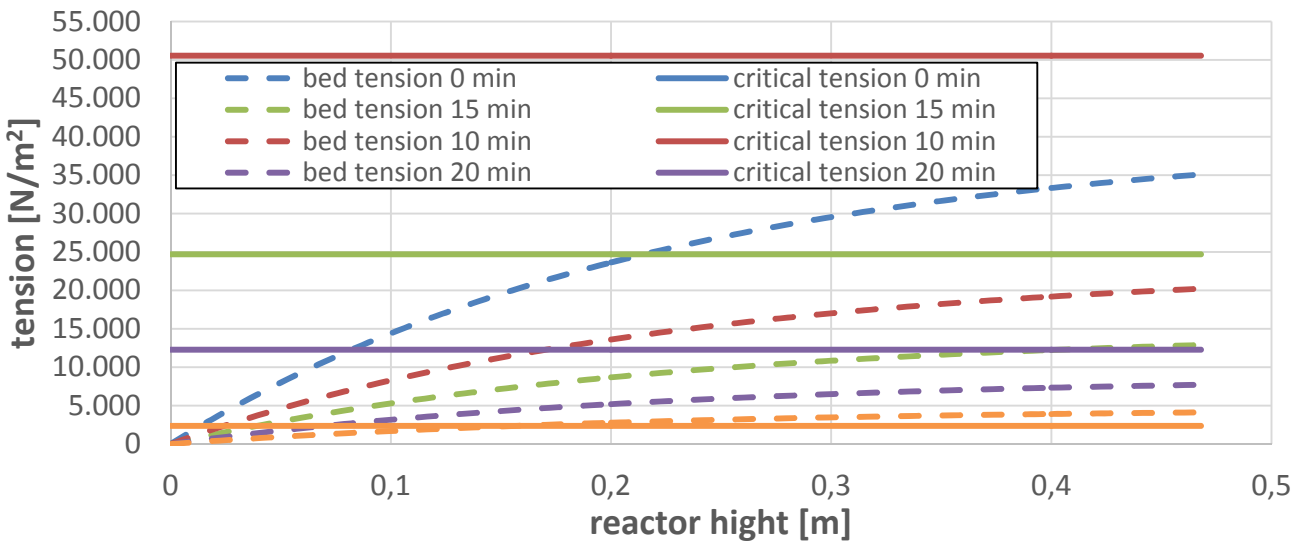


Fig. 3: Simulated bed tension along the reactor height (dashed lines) at different run times; critical bed tensions (full lines) at the same run times from experimental analysis

The model was used to simulate the bed tension along the reactor height, see Fig. 3. It can be seen that the bed tension increases with the height. That is due to the accumulative effect the pressure drop has on the biomass in flow direction. With ongoing time both, the bed tension and the critical bed tension decreases, which can be explained by the reduction of solid biomass left in the reactor, causing an increase of the

mean porosity in the reactor. Anyways, the critical tension is only exceeded at $t = 30$ min. Therefore, it can be concluded that the bed starts being compressed at the top of the reactor between a run time of 20 and 30 minutes.

Summary

The mechanical behavior of wheat straw for different LHW treatment times was analyzed in an external material testing machine using a position controlled piston. The axial tension σ_s the bed can take up was found to be independent on the material compositions that occur in the process. It only depends on the compression state, which can be described by the specific bed volume v , the bed density ρ_{bed} or the porosity ε , see eq. (3). If the so-called critical bed tension σ_{cr} is exceeded, the bed will compress.

In a force balance modelling approach the influence of the wall friction, the gravitational force and the pressure drop on the axial bed tension along the height of the reactor was studied. In good comparison to experimental results, it was found that the critical bed tension is only sufficiently high until a certain reaction time of the LHW process, if no stabilization agent is deployed. The model was also used to determine the influence of geometrical, material and process parameters.

A major hurdle to the scale up of the LHW process is mechanical stability of the fixed bed. The development of technical agents to stabilize the straw bed and suitable geometries for a Scale-Up will be studied.

Acknowledgment

I kindly thank the head of the Institute Prof. Smirnova and Wienke Reynolds for the opportunity and discussions for this work. I thank Thomas Steinweger from the *Institut für Zuverlässigkeitstechnik* for the friendly guidance at the material test machine and Sarah Mbeukem for the friendly cooperation.

References

- [1] Reynolds, W., Kirsch, C., Smirnova, I., Thermal-Enzymatic Hydrolysis of Wheat Straw in a Single High Pressure Fixed Bed. *Chemie Ingenieur Technik* 2015, 87, 1305–1312.
- [2] Stieß, M., *Mechanische Verfahrenstechnik 2*, Springer-Verlag, Berlin and London 1994.

Development of a CO₂-intensified decontamination technology to ensure food safety of low water activity food products

Karen Fuchs

Ruhr University Bochum, Universitätsstr. 150, 44780 Bochum, Germany

Fraunhofer Institute for Environmental, Safety and Energy Technology UMSICHT,
Osterfelder Strasse 3, 46047 Oberhausen, Germany

In recent years, product recalls and foodborne diseases have been increasingly associated with low- a_w foods (foods with low water activity) thus disproving the assumption that food with low- a_w is microbiologically safe. The antimicrobial effect of pressurized CO₂ has been already demonstrated on different foods contaminated with different microorganisms. CO₂-treatment with the aim of microorganism reduction seems to be very promising, as pressurized CO₂ reduces bacteria, yeast and fungi at moderate pressures and temperatures. Until now research was conducted mainly on liquid foods. Few studies considered treatment of solid foodstuffs like meat and fish, fresh spinach and alfalfa seeds. Still less research was conducted on low- a_w food. The studies on low- a_w food focused mainly on the reduction-efficiency of microorganisms and seems to be challenging. No comprehensive evaluations of product quality were conducted. Up to now CO₂-studies, referring low- a_w food, focused solely on the reduction efficiency of microorganisms.

Therefore this work addresses »food safety« with the main objective of developing a CO₂-intensified technology for inactivation of microorganisms on food products with low- a_w and simultaneous securing of food quality. The work will validate the reduction efficiency on microorganisms but will also validate the influence of the CO₂-process on the physical, chemical and sensory properties of food.

Low- a_w food products that have been associated with foodborne disease outbreaks and recalls include almonds, peanuts and nut-pastes, dried fruits and vegetables, dried meat, dairy products like powdered milk, dried teas, herbs and spices. This work will first focus on almonds as model matrix.

Acknowledgment

This work is funded by »The Federal Ministry of Education and Research - BMBF«.

Designing a hydrogen compressor for pressure up to 1000 bar with inner cooled walls

Arian Shoshi

Institute of Process Machinery and Systems Engineering,
Friedrich-Alexander-University Erlangen-Nuremberg, so@ipat.uni-erlangen.de

Introduction

Heat generated during the compression process does not just effect the performance, operation and reliability but also the design of the compressor. The goal of this research is to design a safe and functional prototype of hydrogen compressor for max pressure 1000 bar and with minimum heat losses to surrounding. The described compressor is a plunger type with linear operation and always upward. In top of compressor is injected gas (H_2) and separately an amount of liquid which falls downwards as a liquid film and forming a liquid layer in front end of the plunger. This liquid film have a particular importance in heat transfer from compressed gas to the liquid, ensuring cooled walls in order to prevent heating of the suction gas which has a direct effect in reducing volumetric efficiency. Compressed gas together with an amount of hot liquid therefore is pumped out at the end of discharge stroke. Beside the major effect in heat transfer the liquid layer above the plunger helps to prevent high leak losses and minimize the detrimental space at top dead centre nearly zero!

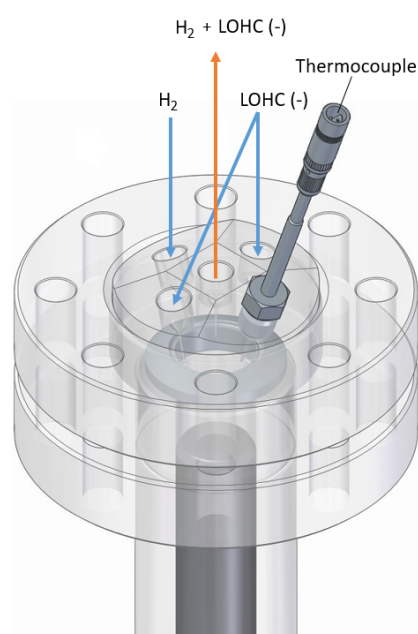


Fig. 1: The upper parts design of compressor

A vast benefit is in hydrogen fuelling stations by applying this type of compressor. A so-called LOHCs (Liquid Organic Hydrogen carriers) are seen as a future application on vehicles. Hydrogen loaded into these LOHCs is non-dangerous and non-flammable. Hydrogenated LOHC require high temperature (need of energy in terms of heat) for dehydrogenation process, at 1 bar the required temperature is round about 300 °C. At ambient pressure they are liquid until 290 °C. LOHCs are well known for its good thermo-physical properties. Taking into account these characteristics LOHCs can be used as a cooling liquid in this type of compressor, therefore this compressor is used for preheating the LOHC which is an important component in hydrogen storage system or hydrogen transport system for making hydrogen available with high pressures and without wasting energy in terms of heat.

Experimental

Due to the high pressure and high temperatures and as well taking into account the medium which is compressed into working chamber, a special materials are to be selected. A-286 (1.4980) is an iron-based alloy commonly used for its combination of high strength and good corrosion resistance at intermediate temperatures~700 °C. Another concern when dealing with hydrogen is hydrogen embrittlement. Iron content in this material perform well in hydrogen service.

The design of compressor is helped by FEA Analysis for some complex shapes (Fig. 2), in order to predict stresses and strains for making a safe design. In the same time there are carried out some heat transfer analysis for assumed temperatures and steady states, but because of the complexity of the two phase flow heat transfer and non-stationary state it's very difficult to predict the discharge temperature of the gas and liquid, therefore a thermocouple is attached direct into the head of compressor to measure temperature during experimental operation (Fig. 1).

The current set-up is under construction and almost at final phase but due to the other components which are required to complete the plant, we couldn't run a test yet. Except the metal construction in a parallel way is built partly a transparent compressor by Plexiglas. In order to find out the behaviour of the liquid into the working chamber, but due to the physical and low mechanical properties of this material the compressor operate relatively at low pressures respectively low temperatures. A high speed camera will be used to investigate the falling film and the layer of the liquid on top of the plunger

under different operation velocity. This will help to optimise the amount of liquid in the chamber.

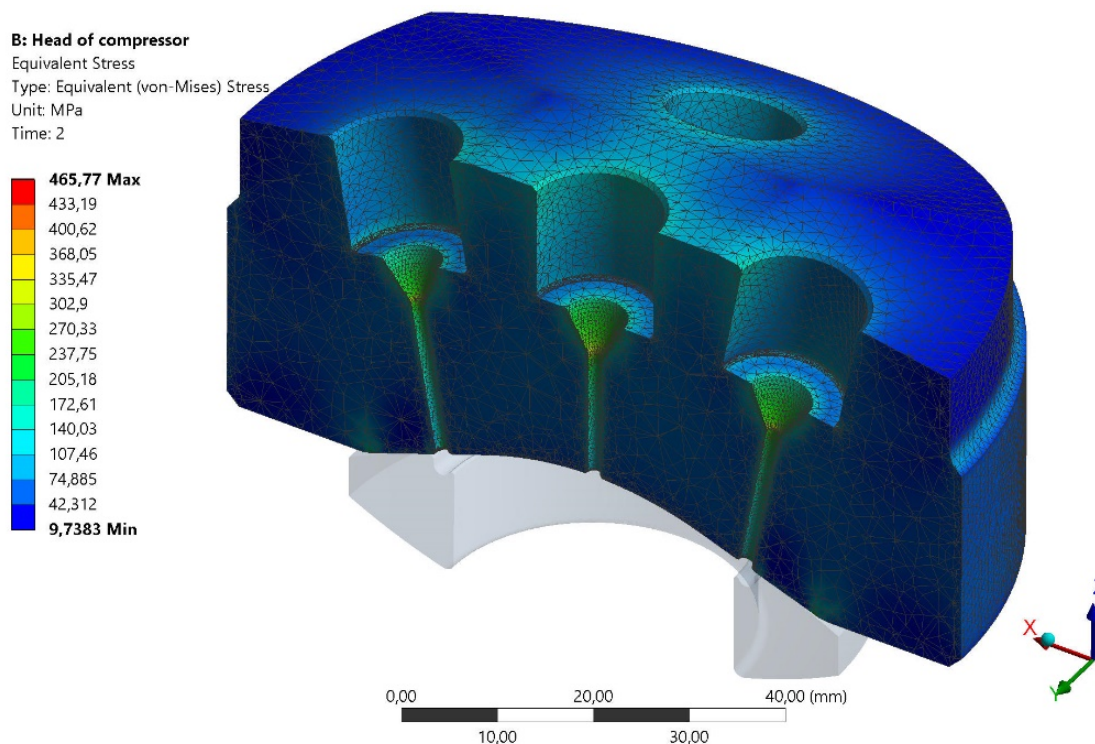


Fig. 2: FEA Stress analysis in the cover (head) of compressor.

Summary

Hydrogen fuel is considered as a promised alternative energy source for future market, hence a much effort is being given in the development of technologies for using it. One example for using hydrogen in fuelling stations and in efficient way was described in this work. The pressures 300 bar and 700 bar are reached until now and the goal is to reach even higher pressures in order to fill with more H₂ fuel in vehicle tanks and in faster way but always safely manner.

Acknowledgment

In order to achieve this goal a special thanks goes to the supporters, KSB Foundation Stuttgart and Energy Campus Nuremberg (EnCN).

References

- [1] A. Bertucco and G. Vetter, High Pressure Technology: Fundamentals and Applications, Elsevier, 2001
 - [2] H. Hugo Buchter, Apparate und Armaturen der Chemischen Hochdrucktechnik, Konstruktion, Berechnung und Herstellung, Springer-Verlag, Berlin / Heidelberg / New York, 1967
 - [3] W. Eifler, E. Schlücker, U. Spicher und G. Will, Küttner Kolbenmaschinen, Wiesbaden: Vieweg+Teubner, 2009.
 - [4] Th. Bergman, A. Lavine, F. Incropera, D. Dewitt. Fundamentals of Heat and Mass Transfer. John Wiley & Sons, 2011
- Linde AG, Hydrogen Technologies, The Ionic Compressors

Redox Properties of Tannins

Gregor Hostnik¹, Maša Knez Hrnčič¹, Martin Gladović¹, Urban Bren¹

¹ Faculty of Chemistry and Chemical Engineering/ Laboratory of physical chemistry and chemical thermodynamics, University of Maribor, gregor.hostnik@um.si

Introduction

Tannins are usually defined as a group of water soluble polyphenols with molar mass between 300 and 3000 g/mol, showing the usual phenol reaction and protein precipitation. Classically tannins are further divided into two subclasses, hydrolysable and condensed tannins (proanthocyanidins). However, according to Khanbabaee and van Ree¹ different division based on their chemical structure can be made.

Gallotannins are tannins, in which galloyl units (or their *meta*-depsidic derivatives) are bound to different polyols, catechin, or triterpenoid units. **Ellagitannins** are those tannins in which at least two galloyl units are CC- coupled to each other and do not contain glycosidically linked catechin units. **Complex tannins** are those tannins in which catechin unit is glycosidically bound to a gallotannin and ellagitannin units. Finally, **condensed tannins** are all oligomeric or polymeric proanthocyanidins, formed by linkage of C-4 of one catechin with C-8 or C-6 of next monomeric catechin.¹ Main structure features of listed groups are shown in Figure 1.

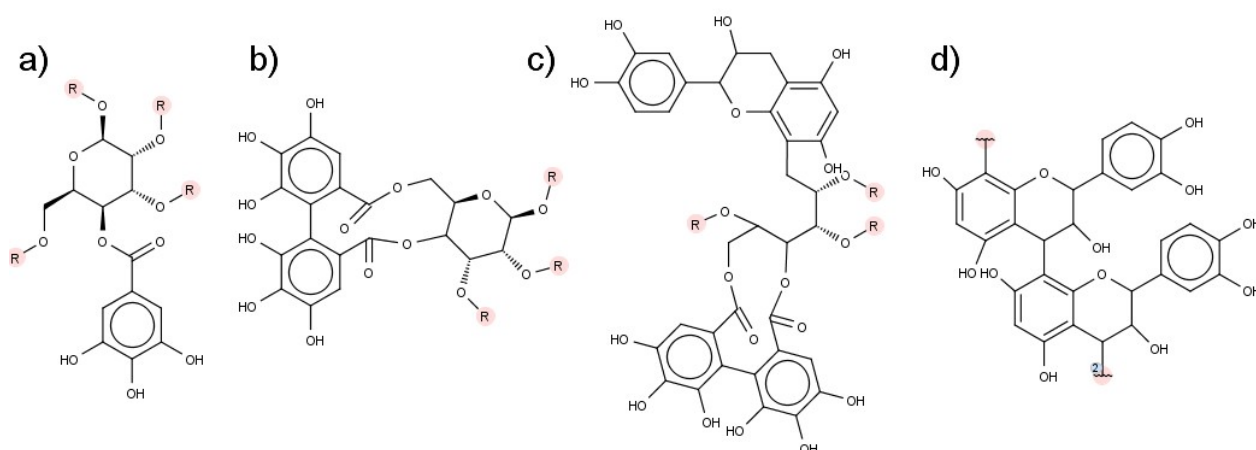


Fig. 1.: Typical structure of: a) gallotannins, b) ellagitannins, c) complex tannins, and d) condensed tannins.

Tannins are present in a vast number of plants and are located in very different tissues. However, they are more common in woody plants than in herbs. It is assumed, that tannins, present in different plant organs have a role of providing their protection against

microbial pathogens, harmful insects and other herbivores, while tannin concentration in tissues is regulated by genetic predisposition and environmental stress.²

Most common and established (probably known from ancient times) usage of tannins is in leather tanning.³ They precipitate saliva proteins. Therefore, they are of bitter and tart taste. Their importance in food industry also cannot be overemphasized. They are either an important factor in taste of red wines or whiskeys or an indicator of undesired sensoric quality of food, which is removed during food processing. In addition they are used as additive in animal feed. Moreover, tannins are, due to their role in plants, subjected to intensive scientific studies as antimicrobial agents. Last but not least, tannins are studied also as compounds, which possibly contribute to human health (decrease the probability of cardiovascular diseases and cancer development, etc.). Even though more or less strong evidence of their health enhancing properties exists, exact mechanism of their action *in vivo* is far from being known and therefore their positive contribution is often disputed.⁴ Nonetheless, it is believed that their possible health enhancing role is connected to their anti-oxidative potential, due to which they might act as free radical scavengers *in vivo*.

In the following work we are going to extract tannins from raw plant material (oak and chestnut wood) and determine the total assay of polyphenols and tannins in the extracted material using ultraviolet/visible spectroscopy (UV/Vis) and high performance liquid chromatography coupled either with UV detector (HPLC) or with mass spectroscopy (LC-MS). Finally the radical scavenger potential is going to be determined experimentally and compared to theoretical predictions.

Three different methods are going to be used for extraction of tannins from oak and chestnut particles: Soxhlet extraction (ethanol, methanol or water; ratio feed/solvent 1/20 (V/V)), ultrasonic extraction (50 °C, 3 h; ratio feed/solvent 1/20 (V/V)), and finally, supercritical fluid extraction by CO₂ with addition of organic co-solvents (5 % ethanol or methanol).⁵ For this type of extraction influence of temperature (40 °C, 50 °C) and pressure (100 bar, 200 bar, 300 bar) on the obtained extract is going to be tested.

The composition of organic components of the extract is going to be determined using LC/MS. Subsequent separation of components will be carried out using sephadex-LH20 as stationary phase while ethanol (for application of sample on stationary phase) and aceton/water (elution of tannins) will be used as mobile phase. Structure of fractions is again going to be again checked using LC/MS.

The radical scavenging potential is going to be determined spectrophotometrically using DPPH (2,2-diphenyl-1-picrylhydrazyl radical) as indicator.⁶

The experimentally obtained results are going to be compared to the results of quantum mechanics calculations. The quantum mechanical calculations are will be performed using Gaussian 16 quantum mechanical software⁷ using various *ab-initio* and DFT levels of theory. With calculation of activation energy barrier (at the beginning for main building blocks of tannins only - gallic acid, ellagic acid, ...) we are going to assess the theoretically predicted viability of tannins for radical scavenging.

Summary

Tannins are very common in many of plants organs, where they play an important role in protection of those organs from different environmental factors. They also play a vital role in technology and human food as well as in animal feed. It is believed that their presence has important influence on human health. An important property that may be crucial for their interaction with body is their redox/radical scavenging potential. In this short abstract an overview of planned activities on a project merging experimental and theoretical research of their antioxidative/redox properties is presented.

Acknowledgment

The study was supported by Slovene Research Agency through the program grant P2-0046 and Republic of Slovenia, Ministry of Education, Science and Sport fund for promotion of scientists at the beginning of their career 2.0

References

1. K. Khanbabaee, T. van Ree, "*Tannins: Classification and definition*", Nat. Prod. Rep., **2001**, 18, 641–649.
2. C. M. Furlan, L. B. Motta, D. Y. A. C. Santos, (**2010**), "*Tannins: What do they represent in plant life?*" In G. K. Petridis, Ed., Tannins: Types, Foods Containing, and Nutrition, New York: Nova Science Publisher, Inc., pp. 265–280.
3. T. Covington (**2009**), "*Vegetable tanning*", In: Tanning chemistry: The Science of Leather, Cambridge: The Royal Society of Chemistry, pp. 281–314.
4. S. Sauer, A. Plauth, "*Health-beneficial nutraceuticals—myth or reality?*", Appl. Microbiol. Biotechnol., **2017**, 101, 951–961.

5. F. J. Barba and Z. Zhu and M. Koubaa, A. S. Sant'Ana, V. Orlie, "*Green alternative methods for the extraction of antioxidant bioactive compounds from winery wastes and by-products: A review*", Trends Food Sci. Tech., **2016**, 49, 96–109.
6. D. Villaño, M. S. Fernández-Pachón, M. L. Moyá, A. M. Tronsoso, M. C. Garcíá-Parrilla, "*Radical Scavenging ability of polyphenolic compounds towards DPPH free radical*", Talanta, **2007**, 71, 230–235.
7. Gaussian 16, Revision A.03, M. J. Frisch, et al., Gaussian, Inc., Wallingford CT, **2016**.

Modelling of High-Pressure Ethene Homo- and Co-Polymerization

P. Peikert, M. Busch

Ernst-Berl-Institut für Technische und Makromolekulare Chemie, Technische Universität
Darmstadt, paul.peikert@pre.tu-darmstadt.de

Introduction

In 2015 more than 322 billion tons of synthetic plastics were produced worldwide.^[1] That large number emphasizes their importance. Living without those materials e.g. in packaging seems to be incredible nowadays. About one third of industrially produced polymers can be assigned to polyethylene (PE) which exhibits a simple polyolefin structure. In dependence on its branching structure polyethylene can be divided into different types. Low Density Polyethylene (LDPE) represents the most commonly produced and consumed plastic material.^[1]

LDPE's unique properties result from its microstructure. Especially feeding a co-monomer, enlarges the possibility to affect macroscopic properties. LDPE and its co-polymers exhibit short-chain branches (SCBs) as well as long-chain branches (LCBs) which are responsible for its outstanding processing properties. In order to predict those properties, the branching structure has to be investigated.

Modelling

Due to its extraordinary process conditions at high-pressures up to 3000 bar and temperatures up to 300 °C polymerization proved to be time and cost intensive.^[2] Therefore product development and process optimization is frequently aided by modelling. Commonly performed simulation of the free radical polymerisation is done numerically. As a result of solving differential equations describing the kinetics as well as balances (heat and impulse) a deterministic simulation only calculates mean values for branching densities. However, if the microstructure is of interest, stochastic modelling, so called Monte-Carlo simulations, are necessary. A stochastic calculation of the individual molecular topology is based on choosing random numbers to determine the sequence of reaction steps resulting in a polymeric chain in the end. *Neuhaus*^[3] developed a coupled deterministic and stochastic simulation approach to model the polymeric microstructure which has been extended by *Eckes*^[4]. The present study is based on that hybrid approach. *Eckes*^[4] validated his model for homo-polymerisations of

ethene in autoclaves as well as in tubular reactors which has been expanded by a copolymerisation approach in this present work. That coupled deterministic and stochastic simulation approach for considering high-pressure ethene co-polymerisations is not limited to a certain co-monomer. Furthermore, reactor modelling is also not restricted to the reactor type. Therefore the microstructure of LDPE-co-polymers being produced in tubular reactors or autoclaves can be determined. The newly developed model is applied to both reactor types and has been validated successfully for an industrial tubular reactor as well as for a 100-mL autoclave. In both cases propene is used as co-monomer. Modelling results exhibit an excellent accordance between deterministically and stochastically calculated mean values (e.g. for branching densities, for co-monomer content). On top of that a new way to store each position of a co-monomer in a chain has been introduced. In combination with storage of the topologic structure it is possible to capture configurational information for ensembles up to 40 million molecules. In consequence of that it is possible to describe the distribution of ethene and the co-monomer which is used. The developed model can then be employed to consider other co-monomers like acrylates or vinyl acetate in order to investigate the co-monomer distribution in the co-polymers. Stored data can also later be used to calculate the radius of gyration in dependence on the chain length or as input for rheological models (e.g. from Read and Leish^[5]).

Summary

A coupled deterministic and stochastic simulation approach for modelling of high-pressure ethene co-polymerisations has been developed and validated successfully for an industrial tubular reactor as well as for a 100-mL autoclave. The hybrid concept is neither limited by co-monomer nor by reactor type. Implementation of a memory efficient way to capture topological information enables evaluation of large molecule ensembles. The stored data can afterwards be used to obtain molecular properties. Besides determining the molecular weight distribution or mean values (e.g. for branching densities) the newly developed hybrid approach can be used to describe the distribution of ethene and co-monomer in the macromolecules. In purpose to obtain a product with defined properties the copolymerisation hybrid approach is an excellent tool to perform simulation aided product design.

References

- [1] PlasticsEurope, **2016**, *Plastics - the Facts 2016: An analysis of European plastics production, demand and waste data*.
- [2] G. Luft, *Chem. Unserer Zeit*, **2000**, 34, 1990-199.
- [3] E. Neuhaus, T. Herrmann, I. Vittorias, D. Lilge, G. Mannebach, A. Gonioukh, M. Busch, *Macromol. Theo. Sim*, **2014**, 23, 7.
- [4] D. Eckes, M. Busch *Macromol. Symp.*, **2016**, 360, 23-31.
- [5] D. J. Read, T. C. B. Leish, *Macromolecules*, **2001**, 34, 10.

Influence of Reaction Time in CO₂ Hydrothermal Reduction

María Andérez-Fernández¹, Eduardo Pérez², Ángel Martín¹, M. Dolores Bermejo¹

¹ High Pressure Processes Group, Department of Chemical Engineering and Environmental Technology, Universidad de Valladolid (Spain)

² TERMOCAL Research Group, Thermodynamics and Calibration, Universidad of Valladolid (Spain)

maria.anderez@alumnos.uva.es

Introduction

In the last decades, atmospheric carbon dioxide (CO₂) emissions have increased due to the anthropogenic activity and have been related to the environmental problems. Several efforts have been developed in order to diminish its atmospheric concentration, such as capture and storage or transformation into value-added chemicals. Conversion of CO₂ in useful fuels and chemicals, e.g. formic acid, methanol and methane, would provide economic benefits as well as sustainable advantages[1]. However, the great thermodynamic stability of CO₂ hinders its transformation, requiring high-energy reactants, such as hydrogen or organometallic compounds[2].

Among the different technologies for CO₂ valorisation, hydrothermal conversion is one of the most promising methods. Hydrothermal processes use high temperature water (HTW), which owns outstanding properties different from those of ambient temperature water, such as lower dielectric constant and higher ion product [3]. Previous studies showed the possibility of reducing CO₂ into formic acid in hydrothermal medium, using metals (Zn, Fe, etc.) or lignocellulosic derivatives (isopropanol and glycerol) as reductants [2,4–6]. A recent study investigated a wide range of lignocellulosic biomass derivatives in order to determine which of them was the most efficient for CO₂ hydrothermal reduction [7]. Almost all the tested compounds showed activity in the conversion of CO₂ to formic acid, being glucose the compound that achieved the highest yield to formic acid (65%).

On the other hand, lignocellulosic biomass is a world-wide spread and sustainable feedstock and it is mainly composed of cellulose, hemicellulose and lignin. These fractions are formed by compounds rich in alcohol groups, which are the main responsible to reduce CO₂ in hydrothermal processes [2]. In addition, glucose is the main component of cellulose. Biomass is envisioned to provide useful bio-fuels and

chemicals in order to reduce the mankind dependence on fossil fuels. Among the different methods to achieve this "green economy", hydrothermal conversion of biomass is considered to be one of the most promising approach. Thus, the combination of both hydrothermal processes of CO₂ reduction and biomass conversion into valuable chemicals could be regarded as an attractive and sustainable strategy for valorization of biomass and CO₂.

In this study, the influence of the reaction time in CO₂ hydrothermal reduction using glucose as reductant is studied in order to optimize the different operational parameters of the process achieving the highest yields to formic acid.

Experimental

NaHCO₃ (100%), as CO₂ source, was purchased from COFARCAS (Spain) while D-(+)-glucose (100%) was acquired from Panreac (Spain). All chemicals were used without further purification treatment. A solution of glucose concentration equal to 0.05M was prepared using ultra-pure water as solvent, while the concentration of NaHCO₃ was 0.50 M.

Reactions were carried out in batch reactors with a length of 12 cm; and an o.d. of ½" with 1 mm of thickness (internal volume equal to 15.6 mL), made of SS 316 stainless steel. The different solutions were introduced in the reactor, filling the 50% of the total internal volume. Then, reactors were placed in an electric oven previously heated to 300°C. After the desired time, reactors were quenched in an ethylenglycol/water bath and liquid samples were collected and analyzed by HPLC.

Results

Figure 1 depicts the yield to formic acid (referring to the initial concentration of glucose) and the conversion of NaHCO₃ at 300 °C performed at different reaction times.

The highest yields to formic acid (65%) were achieved at lower reaction times. However, the yield to formic acid decreased from 30 min to 150 min, where the lowest yield to formic acid was achieved (28 %). Interestingly, the yield to formic acid increased again in the last reaction times tested, achieving yields up to 50% at 190 min. A similar trend is observed in the conversion of NaHCO₃. The highest conversion was reached at the lowest reaction time tested (20% and 10 min, respectively), and it decreased as reaction time increased. Equally to yield to formic acid, the conversion of NaHCO₃

increased again at 150 min, achieving a 19% of conversion at 190 min. In all the experiments, the main by-products obtained were acetic acid, lactic acid, glyceraldehyde, glycolaldehyde and pyruvaldehyde, related to the glucose conversion.

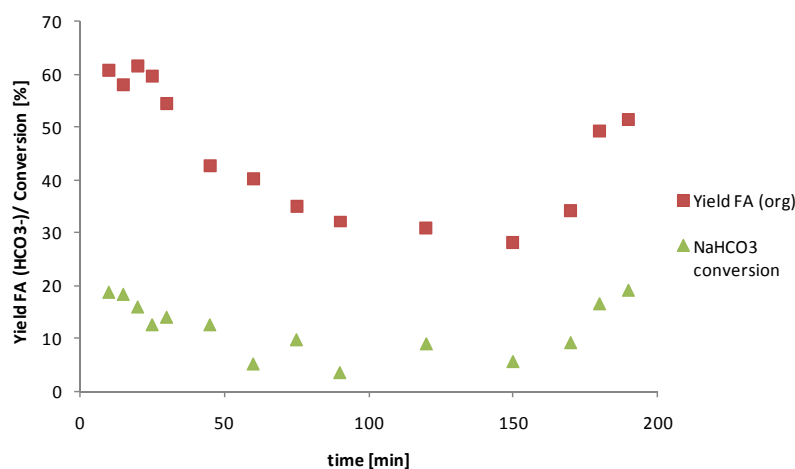


Figure 1. Yield to formic acid and conversion of NaHCO_3 as a function of reaction time.

These results suggest that the CO_2 hydrothermal reduction using glucose as reductant takes place at the first minutes of the reaction, achieving the highest yields and conversions in the firsts 30 minutes of reaction. However, due to the high temperature, the formic acid obtained starts to decompose into CO_2 and hydrogen after this time, decreasing the yield to formic acid and conversion. The increase of yield to formic acid as well as conversion in the last stage of the reaction may be related to the apparition of glucose degradation products, which could react with the CO_2 , reducing it into formic acid again, as previous studies showed [7].

Summary

In this study, a detailed study of temperature influence of CO_2 hydrothermal reduction is shown. The highest yield to formic acid was obtained after 20 min of reaction (62%), while NaHCO_3 conversion was 16% at this time. Despite more insight investigations should be performed should be optimized, this study gives an overlook about the possibility to combine CO_2 hydrothermal reduction with biomass conversion obtaining value-added chemicals and fuels.

Future work will be based on the optimization of different operational parameters (e.g. reactants concentration) in order to optimize the process to obtain higher yields and to implement it in a continuous pilot plant.

Acknowledgment

This project has been funded by MINECO through project ENE2014-53459-R. EPV thanks JCyL for the postdoctoral fellowship. MDB thanks MINECO for Ramon y Cajal position.

References

- [1] M. He, Y. Sun, B. Han, Green carbon science: Scientific basis for integrating carbon resource processing, utilization, and recycling, *Angew. Chemie - Int. Ed.* 52 (2013) 9620–9633. doi:10.1002/anie.201209384.
- [2] Z. Shen, Y. Zhang, F. Jin, From NaHCO₃ into formate and from isopropanol into acetone: Hydrogen-transfer reduction of NaHCO₃ with isopropanol in high-temperature water, *Green Chem.* 13 (2011) 820. doi:10.1039/c0gc00627k.
- [3] N. Akiya, P.E. Savage, Roles of water for chemical reactions in high-temperature water.pdf, *Chem. Rev.* 102 (2002) 2725–2750. doi:http://dx.doi.org/10.1021/cr000668w.
- [4] F. Jin, X. Zeng, J. Liu, Y. Jin, L. Wang, H. Zhong, G. Yao, Z. Huo, Highly efficient and autocatalytic H₂O dissociation for CO₂ reduction into formic acid with zinc, *Sci. Rep.* 4 (2014) 1–8. doi:10.1038/srep04503.
- [5] H. Takahashi, T. Kori, T. Onoki, K. Tohji, N. Yamasaki, Hydrothermal processing of metal based compounds and carbon dioxide for the synthesis of organic compounds, *J. Mater. Sci.* 43 (2008) 2487–2491. doi:10.1007/s10853-007-2041-8.
- [6] Z. Shen, Y. Zhang, F. Jin, The alcohol-mediated reduction of CO₂ and NaHCO₃ into formate: a hydrogen transfer reduction of NaHCO₃ with glycerine under alkaline hydrothermal conditions, *RSC Adv.* 2 (2012) 797–801. doi:10.1039/C1RA00886B.
- [7] M. Andérez-Fernández, E. Pérez, Á. Martín, M.D. Bermejo, Hydrothermal CO₂ using biomass derivatives as reductants, *J. Supercrit. Fluids.* (2017) (submitted).

Encapsulation of Ovalbumin in PLGA Particles through Supercritical Fluid Extraction of Emulsions

Ana Roda^{ab}, Vanessa S. S. Gonçalves^{ab}, Isabel D. Nogueira^c, Ana A. Matias^{ab,*}, Miguel R. Moreno^{d,**}, Subbu Venkatraman^d

^aiBET, Instituto de Biologia Experimental e Tecnológica, Apartado 12, 2780-901 Oeiras, Portugal

^bITQB NOVA, Instituto de Tecnologia Química e Biológica António Xavier, Universidade Nova de Lisboa, Av. da República, 2780-157 Oeiras, Portugal

^cIST, Instituto de Ciências e Engenharia de Materiais e Superfícies, Universidade Técnica de Lisboa, P-1096 Lisboa, Portugal

^dSchool of Materials Science and Engineering, Nanyang Technological University, Nanyang Avenue 639798 Singapore

*amatias@ibet.pt, **miguelramonmorenoraja@gmail.com

Introduction

The encapsulation of proteins and other biomolecules into polymers and lipids for controlled and sustained release purposes has been widely described [1]. The supercritical fluid extraction of emulsions (SFEE) using supercritical CO₂ (sc-CO₂) is an emergent technique for this purpose, by quick removal of the solvent in which the carrier is dissolved, causing its precipitation around the bioactive principle [2]. SFEE allows a continuous and efficient solvent extraction from emulsions by combining the high solubility of organic solvent in pressurized-CO₂ and sc-CO₂ unique properties of permeation. Additionally, the use of a packed column and countercurrent flow of CO₂ promotes an enhanced contact time between sc-CO₂ and the emulsion, improving the solvent extraction and also contributing for the obtention of controlled sizes and narrow size distributions [1,2].

In the present work, the conventional emulsification process was combined with sc-CO₂ extraction for the encapsulation of a model protein, ovalbumin (OVA), in poly(lactic-co-glycolic acid) (PLGA), as a biodegradable, biocompatible and extensively used carrier for sustained release [1]. Its efficiency in terms of solvent removal and control of particle size and particle size distribution was compared with conventional solvent extraction methodology (rotavap).

Experimental

Empty and loaded PLGA droplets were produced by oil-in-water (O/W₂) and water-oil-water (W₁/O/W₂) emulsions, respectively. The emulsion preparation was adapted from [1] using O: PLGA/ethyl acetate (EA) solutions at 10% (w/w); W₁: Poly(vinyl alcohol)

(PVA) 0.04% (w/w) aqueous solutions with OVA concentrations of 10, 20 and 40 mg/mL; W₂: PVA 0.8% (w/w) aqueous solutions. PLGA particles were precipitated by SFEE in countercurrent (apparatus detailed description elsewhere [2]), at 36-38°C, 80 bar or by rotavap coupled to a vacuum controller, at 38°C. The obtained dispersion was washed with water, centrifuged and dried by lyophilisation. The emulsions obtained were analysed by Optical Microscopy (OM) and the efficiency of EA extraction was accessed by gas chromatography (GC). The size, distribution and morphology of the PLGA-particles were analysed by Dynamic Light Scattering (DLS) and Scanning Electron Microscopy (SEM). The load of OVA resultant from SFEE and rotavap was determined by fluorescence spectrophotometry.

Results

The observation of double droplet for W₁/O/W₂ emulsions (OM - data not shown) suggests OVA entrapment in the inner core of the droplets. The residual EA levels varied from 300 to 490 ppm to SFEE and from 650 to 10920 ppm to rotavap, for all the performed experiments, corroborating the higher EA removal efficiency expected for SFEE. Furthermore, the EA residual levels presented by SFEE were much lower than the levels considered safe by the European Pharmacopeia (until 5000 ppm) [3].

Regarding morphology, the PLGA particles precipitated by both methodologies presented spherical shape – figure 1.

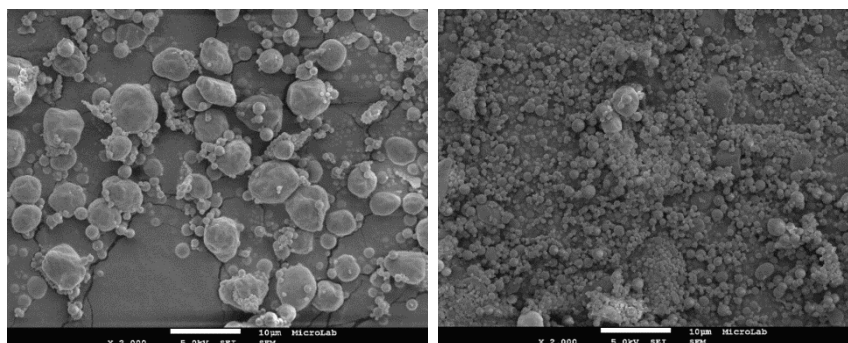


Figure 1.: SEM images of PLGA empty particles, formed by SFEE (right) and rotavap (left) (Scale bar: 10 µm).

The particles sizes were significantly lower and narrower when obtained by SFEE in comparison to rotavap – figure 1 and figure 2 - with no significant size variation when higher OVA concentrations were used – figure 2.

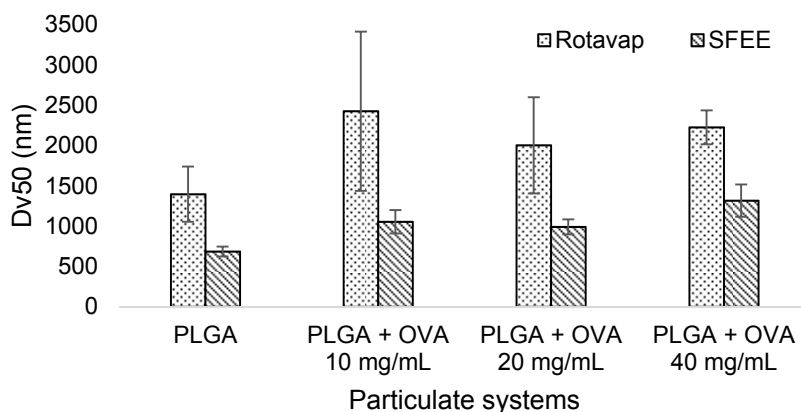


Figure 2.: Median of the particles volume distribution (Dv50) and respective standard deviation (error bars), obtained by DLS.

In terms of load, SFEE showed to be more effective than rotavap for the OVA concentrations tested (data not shown).

Summary

In a perspective of therapeutic applications, SFEE is a preferable process for obtaining lower residual solvent levels, even below the upper limit value considered safe by the European Pharmacopeia (until 5000 ppm) [3] and also for obtaining monodispersed particles with smaller particle size and higher load efficiencies.

Acknowledgment

The authors acknowledge the financial support received from the Portuguese Fundação para a Ciência e Tecnologia (FCT) through the POCI-01-0145-FEDER-016403 project and PEst-OE/EQB/LA0004/2011 grant. iNOVA4Health – ID/Multi/04462/2013, a program financially supported by FCT/Ministério da Educação e Ciência, through national funds and co-funded by FEDER under the PT2020 Partnership Agreement is acknowledged. Ana A. Matias thanks FCT for the financial support through the IF Starting Grant – GRAPHYT (IF/00723/2014).

References

- [1] Falco, N., Reverchon, E., & Porta, G. D. (2013). Injectable PLGA/hydrocortisone formulation produced by continuous supercritical emulsion extraction. *International Journal of Pharmaceutics*, 441(1-2), 589-597.
- [2] Prieto, C., Calvo, L., & Duarte, C. M. (2017). Continuous supercritical fluid extraction of emulsions to produce nanocapsules of vitamin E in polycaprolactone. *The Journal of Supercritical Fluids*, 124, 72-79.
- [3] U.K. European Medicines Agency/ Committee for Human Medicinal Products (2017). ICH guideline Q3C (R6) on impurities: guideline for residual solvents, EMA/CHMP/ICH/82260/2006.

Crystallization of High Porous Metal-Organic Coordination Complexes by the Gas Antisolvent Method

Margarethe Roskosz

Chair of Particle Technology, Ruhr-University Bochum, roskosz@vtp.rub.de

Introduction

Metal organic frameworks (MOFs) turned into an important class of porous crystalline materials. The range of metal compounds and organic linkers leads to a widespread variation in the network coordination and a large variety of properties in the designed MOFs. According to their modifications they outrace conventional porous materials by their specificity. In particular, their high porosity, large surface area and variable internal surface properties make them promising candidates for adsorption, separation, catalysis, chemical sensing and drug delivery [1].

For the investigation of those complex structures, the X-ray single crystal analysis is a good method to determine the arrangement of atoms and their positions in the crystal lattice can be precisely measured and determined.

The challenge consists in the production of single crystals required for the X-ray diffractometer, which, have to show a monocrystalline character and to occur in a minimum size of 100 μm . Conventional crystallization methods have the huge disadvantage that they are time-consuming (weeks to months). [2,3]

The aim of this research is to prepare suitable X-ray single crystals of already known organometallic framework compounds with the gas antisolvent (GAS) method, in which the precipitation of the particles takes place by reducing the solubility with the addition of a gas, in this case CO_2 , as an antisolvent. While solvent and antisolvent are almost



Fig. 1: Single crystals of a Cu-complex.

completely soluble in each another, the solubility of the valuable substance in the antisolvent is very low, therefore the substance is precipitated from the solution as a solid. With this method, it was possible to get for the first time X-ray suitable single

crystals within a few hours (Figure 1). For comparative reasons, all complexes were crystallized by the GAS and a conventional solvothermal method.

The following results of a copper(II) complex are a representative example.

Experimental

Materials

$\text{Cu}(\text{OAc})_2$ was used as metallic component and diethyl cyanomalonate (L) [4] as organic linker (figure 2). Chloroform was chosen as solvent for the conventional and the GAS method. All required reagents and solvents were used without further purification from Merck Millipore Methods.

For the synthesis of the copper(II) complex, 0.1 g of $\text{Cu}(\text{OAc})_2$ and the organic linker in a 1: 2 metal:ligand molar ratio are dissolved in 70 ml chloroform and stirred for 24 h at room temperature. The resulting precipitate is filtered, washed and dried under vacuum for 12 h.

Gas antisolvent crystallization. The crystallization under CO_2 as antisolvent is carried out in a high pressure view cell. The autoclave was treated with a saturated solution of the copper complex in chloroform at a reaction time of 3 h, a pressure of 100 bar and a temperature of 40 °C. After the indicated reaction time, the autoclave is purged at a constant pressure of 100 bar for 45 min with CO_2 . Finally, the view cell was slowly depressurized over 3 h.

Conventional crystallization. Single crystals of the copper(II) complex were also obtained by a conventional crystallization method. For this purpose, a concentration series is obtained from the saturated solution in chloroform and placed in a sealable glass vessel filled with diethyl ether. Subsequently the glass vessel is sealed and placed in a place free of mechanochemical influences. After 24 h the first crystals can be seen.

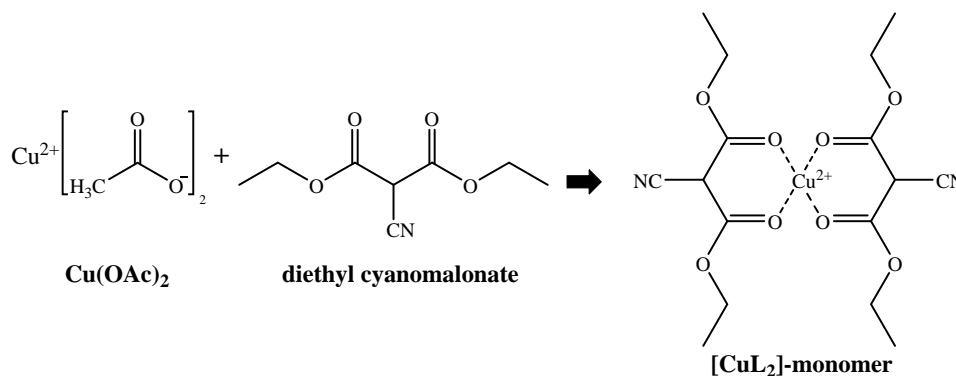


Fig. 2: Formation of metallic component, $\text{Cu}(\text{OAc})_2$, and organic linker, diethyl cyanomalonate, to $[\text{CuL}_2]$ -monomer.

Summary

The products of both crystallization methods are obtained as green crystals with a minimum size of 100 μm , which is required for the diffractometer. For the structural analysis, intensity data sets were determined, using a single crystal X-ray diffractometer (Stoe IPDS I) with graphite-monochromatic $\text{MoK}\alpha$ -X-ray radiation. The analysis of these data sets showed, that the obtained structures from both crystallization methods are isotype to each another.

The copper(II) complex is obtainable as a one-dimensional coordination network, build up from monomers of the composition $[\text{CuL}_2]$ (figure 3).

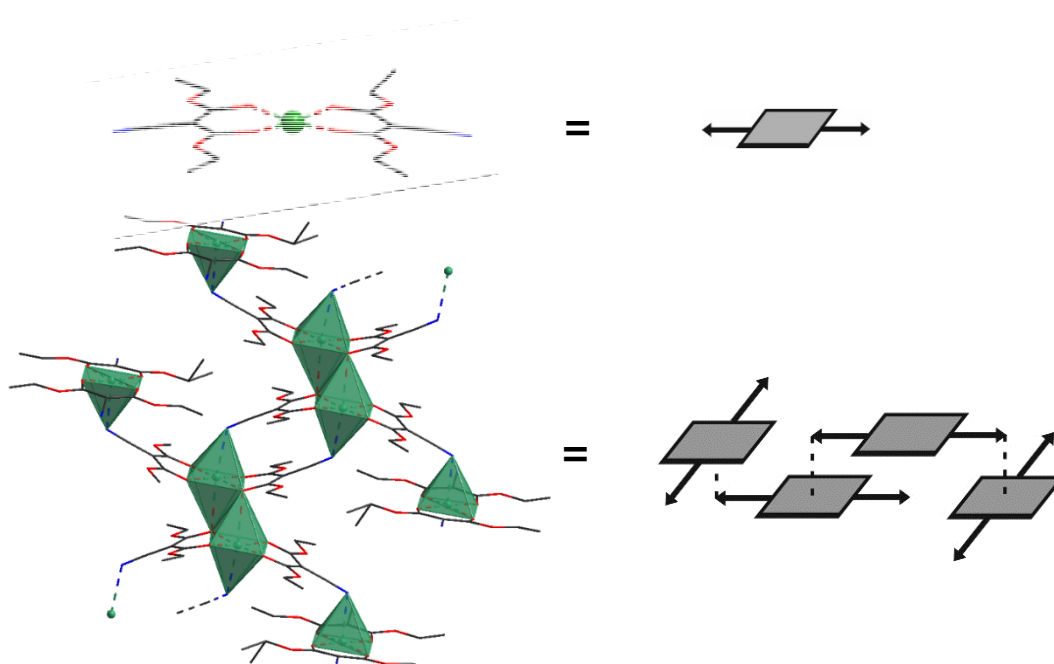


Fig. 3: $[\text{CuL}_2]$ -coordinated chain-like crystal structure to $[\text{CuL}_2]_n$. Coordination groups colored: carbonyl group = red and cyano group = blue. H-atoms are not displayed for clarity.

Regarding to this monomer, in the equatorial position, two organic ligands coordinate bidentately over their carbonyl groups to the copper(II) center and form a $[\text{CuL}_2]$ -monomer. The coordinative interaction among those monomers occur over the carbonyl and cyano groups of the ligands, what leads to a slightly distorted bipyramidal coordination (figure 3). The arrangement of several monomers to a coordination network is possible because the copper(II) atom is coordinative unsaturated before the attachment of the ligands in the axial positions. This occupation leads to a chainlike arrangement. The coordination polymer of the type $[\text{CuL}_2]_n$ crystallizes by self-organization in the triclinic space group $P\bar{1}$.

References

- [1] D. Zhao et al, *Acc. Chem. Res.*, 2011, vol. 44, pp. 123–133.
- [2] L. Li et al, *CrystEngComm*, 2013, vol. 15, pp. 4094-4098.
- [3] M. O. Rodrigues, et al, *Int. J. Quantum Chem.*, 2012, vol. 112, pp. 3346–3355.
- [4] M. Roskosz, *Charakterisierung und CO₂-unterstützte post-synthese Behandlung metallorganischer Koordinationskomplexe*, master thesis, Bochum, 2015.

Lignin Valorization by Hydrolysis in Supercritical Water

Tijana Adamović

Department of Chemical Engineering and Environmental Technology, University of
 Valladolid, tijanaadamovic@gmail.com

Introduction

Lignin, together with cellulose and hemicellulose, is the principal component of plants that have function to assist in the movement of water. Lignin is a polymer, built up by the combination of three basic monomer types that differ in the substitution at the 3 and 5 position, as shown in the figure 1. The compositions of lignin polymers are unique to each species of plant. For example, the principal monomer for softwood lignins is coniferyl alcohol, which has a methoxyl group on the C-3 position. Hardwood lignins have two main monomers: coniferyl alcohol and sinapyl alcohol, which has methoxyl groups on both the C-3 and C-5 positions. The third monomer, *p*-coumaryl alcohol, is more prominent in grasses and compression wood. The aromatic rings of the monomers are often referred to as follows: guaiacyl units have one aryl-OCH₃ group and are derived from coniferyl alcohol, syringyl units have two aryl-OCH₃ groups and are derived from sinapyl alcohol, and *p*-hydroxyphenyl units have no OCH₃ groups and are derived from *p*-coumaryl alcohol [1]. Therefore, phenolic chemicals could be obtained from lignin by chemical degradation processes.

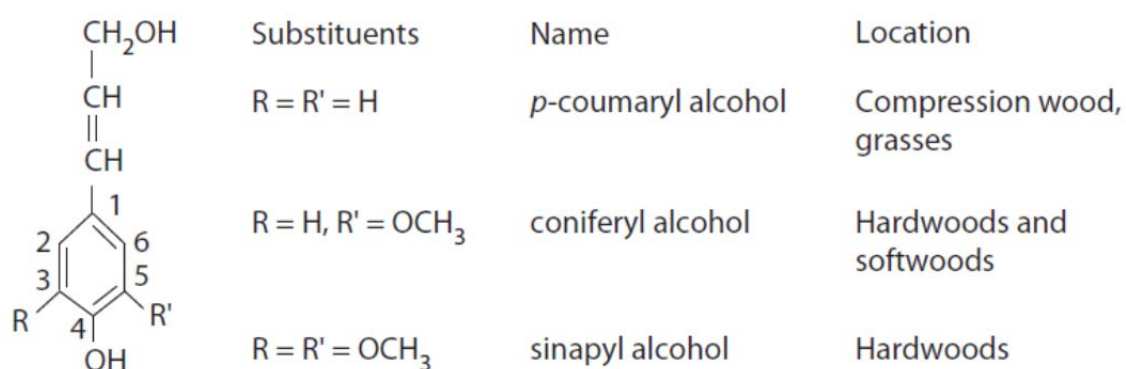


Figure 1. Lignin monomeric building blocks

High temperature water (HTW) which is defined as liquid water above 200°C and supercritical water (> 374°C and 218 atm) is attracting attention as a medium for organic chemistry. HTW and SCW exhibits properties that are very different from those of ambient liquid water [2]. The absence of phase boundaries at supercritical conditions allows many reactions to proceed homogenously with few mass transfer limitation. The

completely miscibility of SCW with gases and organic compounds makes SCW an excellent solvent for oxidations, hydrogenations and hydroformylations [3]. Near critical point properties of water can be highly influenced by changing pressure and temperature what mean that identity of the medium can be modified without changing the solvent [4]. This behavior is a promising alternative to control the selectivity in chemical reaction. The main reactions pathways that have been identified in SCW are those with an ionic or radical character. Reactions seem to proceed via ionic pathways in liquid water, high pressure SCW and probably the dense gas phase. In contrast, radical reactions seem to be the main reaction pathways in steam and less dense SCW. Both reactions proceed competitively around the critical point of water [3]. Because of its unique properties HTW and SCW has received attention as a reaction solvent for biomass. The decomposition of lignin and lignin model compound was studied under those conditions. Lignin seems to follow a first depolymerization step that is favored at high temperature. However, the residence time is very important at this point because the formed products (mainly guaiacol) can react with higher molecular weight compounds to form new polymers, called phenolic char [5–7].

Chemical reactivity in supercritical fluids has been investigated widely by traditional methods, which normally involve chemical analysis of the reaction mixture after it has been returned to ambient temperature and pressure. The use of optical spectroscopic methods, however, allows one to probe reactions in an in situ fashion and should yield more detailed insight into chemical interaction. Raman spectroscopy is a versatile diagnostic tool that has been applied widely in gas, liquid, and solid media. Compared to other optical techniques, Raman spectroscopy is well suited to supercritical fluids because it is immune to quenching at high pressures (or densities) and because it allows easy access to broad spectral ranges. Solvated molecules can usually be identified by their distinct Raman shifts, unless the overlap of features becomes severe [8].

Experimental

The study is carried out in The High Pressure View Chamber Type HPVC 300-HT that is designed for observation of phase behavior and reactions at elevated temperatures and pressures (figure 2). It is designed to operate up to 30 MPa and 500°C. Basically, a cylindrical internal volume is filled with a fluid. Two cylindrical shaped sapphire windows that are allocated opposite to each other allow visualization of main

part of the cylinder internal volume. A manually operated magnetic lift allows to place a solid sample inside the view chamber after being thermostated and pressurized via sluice (lock hopper) system. Two further ports allow fluid supply, sampling and pressure detection.



Figure 2. The High Pressure View Chamber Type HPVC 300-HT

Summary

The biomass exploitation as raw material is recognized as an alternative for the sustainable production of fuels, materials and different chemicals. Among lignocellulosic biomass components, nature aromatic polymer lignin is the second most abundant polymer. Thus, lignin revalorization into high added value platform chemicals could improve the profitability and diversity the production of the future biorefinery.

High temperature pressurized water has proved as a good solvent for clean, safe and environmentally benign organic reaction. The different properties of pressurized water depending of its pressure and temperature can be adopted in order to choose medium where highest selectivity of chosen compound could be obtained.

The gold of this thesis is to improve understanding of lignocellulosic biomass fractionation by a fundamentals study about lignin dissolution / hydrolysis in sub / supercritical water, and its validation with the corresponding kinetic studies in ultra-fast reactors. Special design of visual cell allows in situ Raman analysis and following the dissolution / hydrolysis and lignin re-polymerization reactions from the start of the reaction.

Acknowledgment

Thanks to MINECO and FEDER program for the financial support Projects CTQ2013-44143-R and CTQ2016-79777-R.

References

- [1] B. Raton, L. New, F. Group, Lignin and Lignans Advances in Chemistry, n.d.
- [2] N. Akiya, P.E. Savage, Roles of Water for Chemical Reactions in High-Temperature Water, *Chem. Rev.* 102 (2002) 2725–2750.
- [3] M. Watanabe, T. Sato, H. Inomata, R.L. Smith, K. Arai, A. Kruse, E. Dinjus, Chemical Reactions of C 1 Compounds in Near-Critical and Supercritical Water, *Chem. Rev.* 104 (2004) 5803–5822. doi:10.1021/cr020415y.
- [4] D.A. Cantero, M.D. Bermejo, M.J. Cocero, Governing Chemistry of Cellulose Hydrolysis in Supercritical Water, *ChemSusChem.* 8 (2015) 1026–1033. doi:10.1002/cssc.201403385.
- [5] Z. Fang, T. Sato, R.L. Smith Jr., H. Inomata, K. Arai, J.A. Kozinski, Reaction chemistry and phase behavior of lignin in high-temperature and supercritical water, *Bioresour. Technol.* 99 (2008) 3424–3430. <http://www.sciencedirect.com/science/article/pii/S0960852407006311>.
- [6] T.L.-K. Yong, Y. Matsumura, Kinetic analysis of lignin hydrothermal conversion in sub- and supercritical water, *Ind. Eng. Chem. Res.* 52 (2013) 5626–5639.
- [7] T.L.-K. Yong, Y. Matsumura, Reaction Kinetics of the Lignin Conversion in Supercritical Water, *Ind. Eng. Chem. Res.* 51 (2012) 11975–11988. <http://pubs.acs.org/doi/abs/10.1021/ie300921d>.
- [8] D. a Masten, B.R. Foy, D.M. Harradine, R.B. Dyer, In situ Raman spectroscopy of reactions in supercritical water, *J. Phys. Chem.* 97 (1993) 8557–8559. doi:10.1021/j100135a003.

Inline-Pulsation-Damper for Reduction of Pressure Pulsation in a Triplex Diaphragm Pump

Daniel Steger

Institute of Process Machinery and Systems Engineering, Friedrich-Alexander-University
Erlangen-Nuremberg, sg@ipat.fau.de

Introduction

Positive displacement pumps are significantly more efficient than centrifugal pumps. But their mode of action causes more pressure pulsation than other working principles. That means that the utilization of positive displacement pumps requires to concern pulsation damping [1, 2]. At the Institute of Process Machinery and Systems Engineering (iPAT) at Friedrich-Alexander University Erlangen-Nuremberg energetically efficient and economically optimized design concepts for pumping systems are developed. One research aspect is an effective dampening of pressure pulsations at the discharge side as well as at the suction side, working flexible at high, medium and low pressure and as close as possible to the place of their origin. Achieving these goals will spread the field of applications for positive displacement pumps and thus generate chances for increasing the energetic efficiency of process engineering systems.

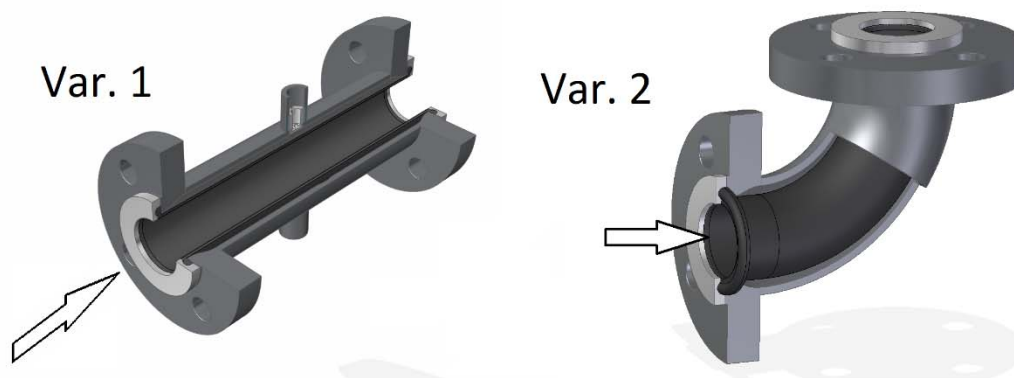


Fig. 1: Two Variants of Inline-Dampeners

In order to realize a pulsation-free operation of positive displacement pumps, a new damper system is developed for easy integration into the pump module [3]. The inline-pulsation-damper consists of a simple pipe section, into which a hose is inserted (Fig. 1. Var. 1). The space between the pipe and the hose is filled with pressurized gas. If a pulsating flow passes this damper, the amplitudes are absorbed by the gas compartment via the membrane. The gas pressure can be adjusted via a control valve which is designed to adapt the best conditions of damping automatically and self-

adaptive. This system meets the pumps special requirements and can be designed to operate at all pressure conditions.

Experimental

The experimental setup to evaluate the damper consists of a positive displacement pump, which is a triplex diaphragm pump, a backpressure valve to adjust the pressure and the corresponding piping system. Due to the pressure conditions, several safety relevant devices had to be constructed, such as the hose protection plug. Three Inline-Dampers are located directly at the three discharge valves of the pump (Fig. 2) and besides there is the possibility to switch on a bladder accumulator at the discharge side.



Fig. 2: The triplex diaphragm pump with three inline-pulsation-dampers

The tests are performed with several pump speeds (50...200 rpm) and pressure levels (up to 40 bar) for different configurations of the test setup (without any damping, inline-pulsation-damper in use; bladder accumulator in use, combined damping).

The results show the inline-pulsation-damper being very useful for both reducing the pressure pulsation and smoothing the volume flow. Pulsation with frequencies above 20 Hz can be almost completely suppressed. Fig. 3 shows the pressure in the pumped medium as well as in the gas compartment of the damper recorded over a period of 300 s. Moreover, the Pulsation on the discharge side was measured and is shown as well. One can now easily recognize: Adapting the pressure level in the damper to the

pressure level of the medium significantly lowers the pulsation of the discharge pressure. Thus, amplitudes of up to 5 bar can be reduced to less than 0.2 bar.

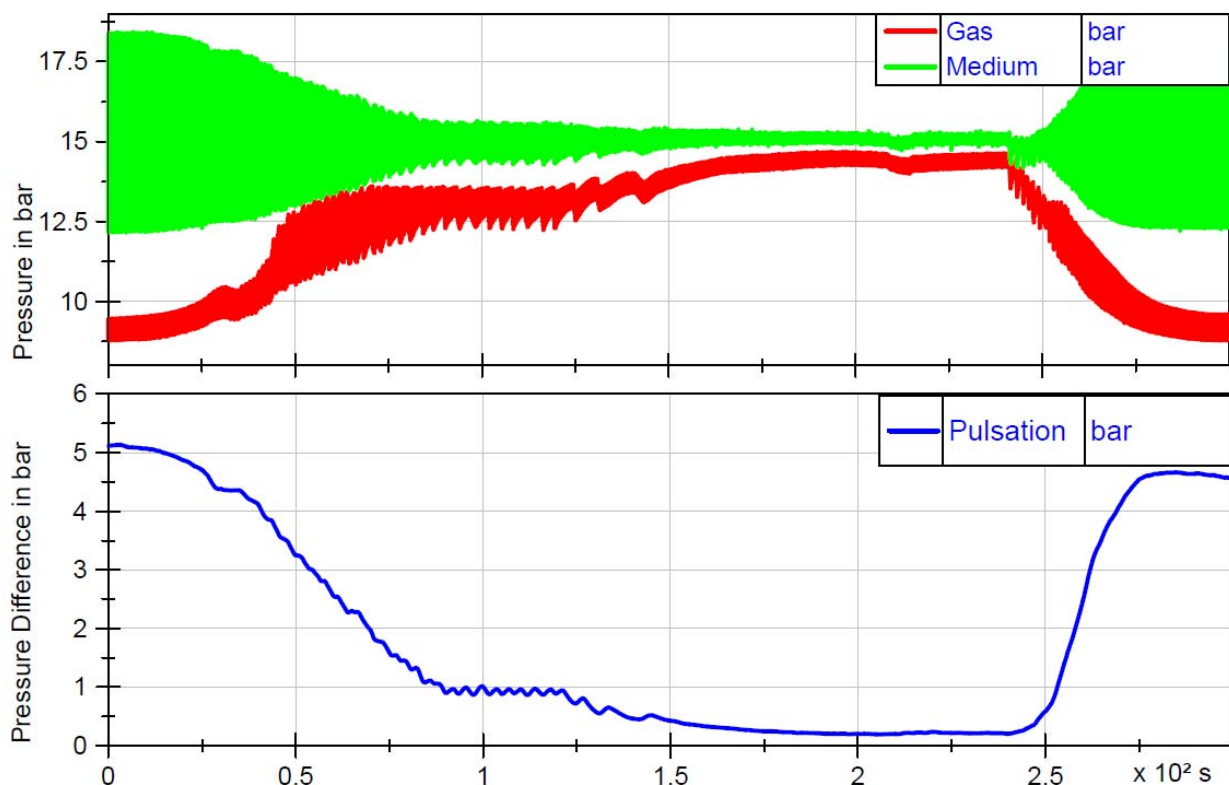


Fig. 3: Reducing the Pulsation by using the inline-pulsation-damper at 168 rpm

While the bladder accumulator seems to be more useful for damping lower frequencies it fails at higher ones. In some cases, even a worsening of the acoustic pressure pulsations close to 50 Hz has been recorded. For damping the unsteadiness of the flow rate both types of dampers seem to be applicable, the bladder accumulator being slightly more effective.

Summary

The studies at the triplex process pump have shown that the inline damping concept can be easily integrated to the pump module. Pressure pulsation, as well as structure-borne noise, can be reduced substantially. The inline-pulsation-damper is a good alternative to the bladder accumulator especially for damping high frequencies. It provides even more benefits, like a flexibility to changing system conditions by adapting the gas pressure and the opportunity of being cleaned in place (CIP). Furthermore, transferring the principle into a pipe bend (Fig. 1. Var. 2) might reduce the impact of a water hammer and protect the plant against serious damages.

Acknowledgment

Thanks to the Federal Ministry for Economic Affairs and Energy Germany for supporting the project.

References

- [1] G. Vetter, Rotierende Verdrängerpumpen für die Prozesstechnik, Essen: Vulkan-Verlag, 2006.
- [2] W. Eifler, E. Schlücker, U. Spicher und G. Will, Küttner Kolbenmaschinen, Wiesbaden: Vieweg+Teubner, 2009.
- [3] A. Kögler, D. Haselmann, N. Alt und E. Schlücker, Experimental Characterization of a Flow-through Pulsation Damper Regarding Pressure Pulsations and Vibrations, Chemical Engineering Technology, 2016.

Synthesis of Stationary Phases for Chiral Separations and Thermodynamic Studies of Adsorption by Supercritical Fluid Chromatography

Miaotian Sun, Pavel Gurikov, Irina Smirnova, Monika Johannsen

Institute of Thermal Separation Processes, Technical University of Hamburg

m.sun@tuhh.de

Introduction

2-Arylpropionic acid derivatives (2APAs-profens) are an important subgroup within the class of nonsteroidal anti-inflammatory drugs (NSAIDs). They are prepared in a racemic mixture but usually only a single enantiomer is pharmacologically active. Therefore, the enantiomeric separation of this group of chemicals is of great importance in pharmaceutical industry. The attempt made in this work is to synthesize different chiral adsorbents to be used as stationary phases for chromatography. The products obtained by these methods have been investigated in static adsorption experiments.

Furthermore, SFC process becomes a predominate method for chiral separations in recent years. Thanks to the high diffusivity and low viscosity of supercritical CO₂, the resolution has been improved and the process time has been reduced. Meanwhile, chromatography is also a powerful tool to carry out fundamental studies on the interaction of solutes with solid materials. However, the knowledge to carry out these studies with SFC is so far quite limited when compared to those with GC and HPLC. Therefore, another motivation of this work is to develop and validate a method for comprehensive study of the interactions and adsorption behavior within the complex SFC system consisting of supercritical CO₂, co-solvent, solutes and solid materials.

Experimental

Synthesis and characterization of chiral adsorbents

Three methods were applied in this work to synthesize chiral adsorbents. By the first method, commercial chromatographic silica gels were modified with (S)-ibuprofen by covalent bonding through a spacer, 3-glycidoxypropyl-trimethoxysilane [1]. By the second co-gelation method, (S)-ibuprofen was encapsulated during a gelation process with tetraethyl orthosilicate (TEOS) and (3-aminopropyl)triethoxysilane (APTES) [2] and dried by supercritical CO₂ afterwards. By the third method, molecular imprinted polymers (MIPs) were synthesized by a multi-step swelling and redox polymerization method

using polystyrene as shape template, 4-vinylpyridine as monomer, ethylene dimethacrylate as cross-linker and ibuprofen or naproxen as template [3].

The chiral selectivities of the synthesized materials were determined in batch adsorption experiments. The selectivity index S_R was calculated from distribution coefficient D as follows:

$$D = \frac{Q_e}{c_e}; S_R = D_R/D_S.$$

Here Q_e and c_e are the ibuprofen loading and concentration at equilibrium. The adsorption isotherm of the material synthesized by the first method is given in Fig. 1 (left panel). As predicted, there is no chiral selectivity from unmodified silica, but small differences between the loadings of (R) and (S)-ibuprofen on modified silica can be observed. However, the values of selectivity index among all three kinds of silicas are very low, which are in a range of 0.95 to 1.09.

Higher chiral selectivities were achieved by ibuprofen-encapsulated silica. As seen from Fig. 1 (right panel), the large differences between the loadings of two enantiomers indicate good selectivities, which are ranging from 1.32 to 1.76.

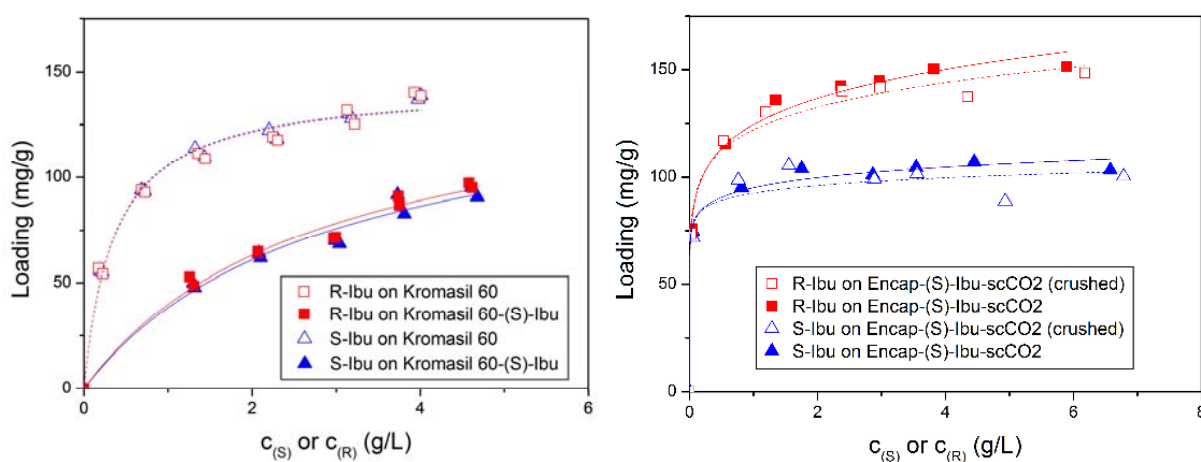


Fig. 1.: Left: Adsorption isotherms of R/S-ibuprofen in n-hexane on chemically modified and unmodified silicas at 20 °C fitted in Langmuir model. Right: Adsorption isotherms of R/S-ibuprofen in n-hexane on ibuprofen-encapsulated silica at 20 °C fitted in Freundlich model.

Mixed retention model

A mixed retention model has been applied to describe the retention behavior of solutes on selective stationary phases. The theory behind this model is that the retention of a solute is due to a mixed retention mechanism of the adsorption of the solute on the free silanol groups as well as its adsorption on the adsorbed modifier molecules, which can be written as:

$$k_{obs} = k_0(1 - \theta) + k_c\theta$$

where k_0 is the contribution of silanols to retention at zero concentration and k_c is the contribution of adsorbed modifier molecules at full coverage. θ refers to the surface coverage by the modifier and has been determined by frontal analysis within this work. A breakthrough curve obtained for frontal analysis is shown in Fig.2 (left panel). Adsorption isotherms can be obtained by calculating the overall mass balance through the breakthrough curve by the following equation:

$$V_{plant} \cdot c_2 + V_c \cdot [\varepsilon_t \cdot c_2 + (1 - \varepsilon_t) \cdot q(c_2)] = \dot{V} \cdot c_2 \cdot (t_{inflexion} - t_{inject})$$

where V_{plant} is the dead volume of the SFC plant. V_c is the volume of the column. ε_t is the porosity of the column. c is the modifier concentrations and q is the corresponding loading.

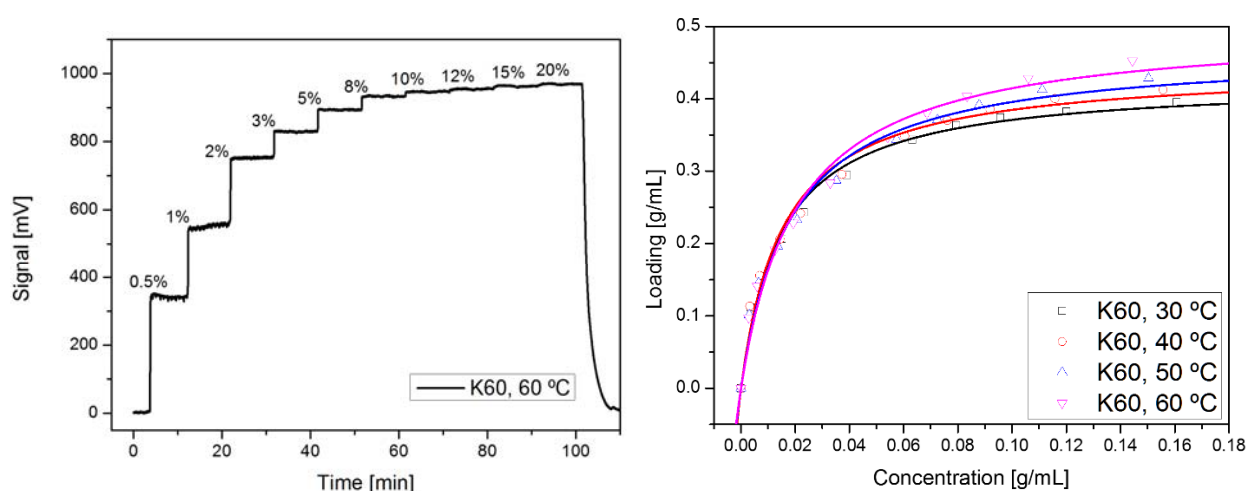


Fig. 2.: Left: Breakthrough curve obtained for frontal analysis of methanol adsorption on silica K60 in supercritical CO_2 at 200 bar. Right: Adsorption isotherms of methanol on Kromasil K60 in supercritical CO_2 at 200 bar at various temperatures fitted in Langmuir model.

The adsorption isotherms of modifier (methanol) on a commercial chromatographic silica gel Kromasil 60 Å (K60) in supercritical CO_2 at back pressure of 200 bar at various temperatures are shown in Fig.2 (right panel). The experimental data were fitted in Langmuir isotherm model and θ values were determined afterwards to be applied in the mixed retention model. An example of experimental data from SFC experiments fitted by the model is shown in Fig. 3. The model shows great agreement with the experimental data and k_0 s were predicted through it. The k_0 is a critical parameter due to the fact that it cannot be determined directly through experiment because the using of modifier cannot be avoided to elute polar solutes from a polar solid matrix in SFC. Further

thermodynamic information, such as adsorption enthalpy and entropy, can be extracted as well through the parameters of the model.

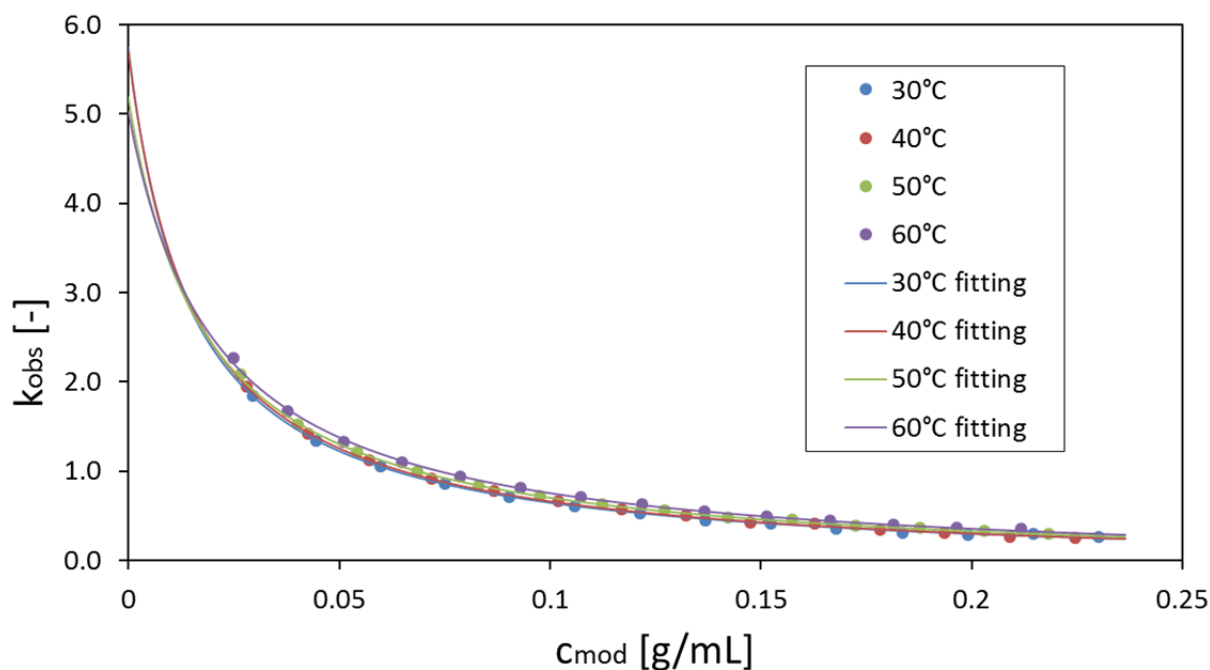


Fig. 3.: Observed capacity factor of phenol on Kromasil K60 at different concentrations of modifier obtained by SFC experiment at 200 bar fitted in mixed retention model.

Summary

Three different methods have been carried out to produce chiral materials aiming to be used as stationary phases in SFC. The products were characterized and good chiral selectivities were achieved by the (S)-ibuprofen encapsulated silica in adsorption process. Mix retention model has been validated through SFC experiments and further information can be extracted from the model for deeper understanding of the complex system in SFC.

References

- [1] Tourné-Péteilh *et al*, *New J. Chem.* **2003**, 27, 1415-1418.
- [2] Qu *et al*, *Eur. J. Inorg. Chem.* **2006**, 3943-3947.
- [3] Haginaka *et al*, *J. Chrom. A* **1998**, 816, 113-121.

Biopolymer Foam Extrusion – Modelling CO₂ Dispersion and Dissolution Phenomena in High Viscous Polymer Melts

Judith Janowski

Institute of Thermo and Fluid Dynamics, Ruhr-University Bochum, Germany

janowski@vvp.rub.de

Introduction

Polymer Foams offer various features such as low weight, high cushioning and insulation efficiency. Polylactic acid (PLA), a bio-based and biodegradable biopolymer, is a proven material for manufacturing microcellular foams. Supplemented by the use of supercritical CO₂ as physical blowing agent, both the foaming process and the biopolymer foam product are eco-friendly and sustainable. [1]

Continuous foaming processes are carried out by extrusion units. Compressed CO₂ is injected into the extruder barrel, dispersed and dissolved into the polymer melt. The mixture is conveyed to the extrusion die, where the pressure drop induces thermodynamic instability and cell nucleation. Depending on the operating pressure and temperature, cell growth and foam stabilization occurs. Therefore, the foam density and morphology is caused by various operating parameters. Beside the individual material properties, the characteristics of polymer foams are primarily affected by the foam morphology. To obtain a low-density foam consisting of small, homogeneous pores, the mixture of PLA and CO₂ has to be well homogenized inside the extrusion unit and effectively cooled down towards the die, at about the solidification temperature of the polymer. Therefore, current research focusses on precise control of foaming mechanism. [2]

Experimental

To model the CO₂ transport phenomena inside high viscous polymer melts, two sub-areas are investigated. Initially, the discontinuous foaming process using a pressure vessel is observed. Here, the gas dissolution is based on diffusion on the molecular level. In the second part, the continuous foaming using an extruder is focussed. In this case, gas dispersion occurs additionally to dissolution. This is conditioned by the driven extruder screws and the following flow velocities and shear rates.

For both parts, the PLA grade Ingeo 2003D from NatureWorks LLC (USA) is used. In table 1 the material parameters of the PLA resin are listed. Carbon dioxide with a purity of 99.9 % is supplied by YARA GmbH & Co. KG.

Tab. 1: Material parameters of 2003D PLA

Property	Value
Density	1.24 g/cm ³
MFR (210°C,2.16 kg)	6 g/10min
M _w	210 000 g/mol
D-lactide content	4.25 %

The foamed samples are characterised by several factors. The expansion ratio is calculated by comparing the initial polymer volume with the foam volume. Supplementary, the cell morphology is determined by using a scanning electron microscope.

The discontinuous foaming experiments using a pressure vessel are preliminary for the continuous ones. Therefore, the discontinuous foaming process is using similar conditions like the ones used in the continuous process. So, PLA granules are heated first, then loaded with compressed carbon dioxide. After soaking, the gas-enriched polymer melt is cooled down while still at enhanced pressures, and the decompression step is subsequently performed.

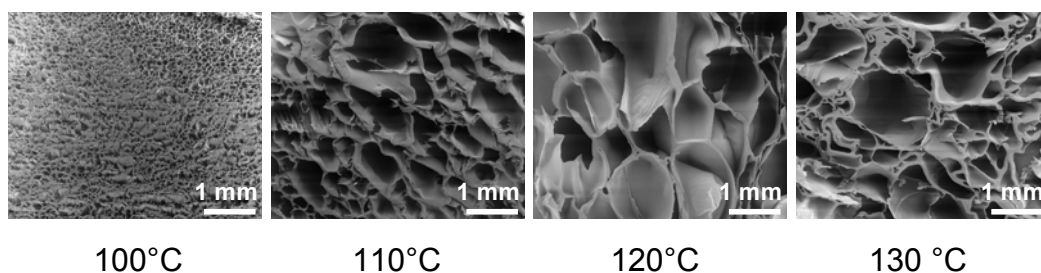


Fig. 1: Cell morphology at various foaming temperatures

The foamed samples show a closed-cell morphology with expansion ratios of around 7. Depending on the operating temperature, deviations of the foam morphology are shown in figure 1. At 100 °C, the cell density is high and decreases with increasing temperature. This is caused by the gas diffusion inside the polymer melt. At higher temperatures, it takes more time until the polymer solidifies. Thus, more cell growth and coalescence occurs.

In figure 2, the continuous foam extrusion scheme is illustrated. The transport mechanisms inside extrusion units are affected by gas dissolution as well as the dispersion of the gaseous phase. Highly dispersed small gas bubbles create an enhanced surface for mass transfer, which leads to a quicker dissolution of the gas into the polymer phase.

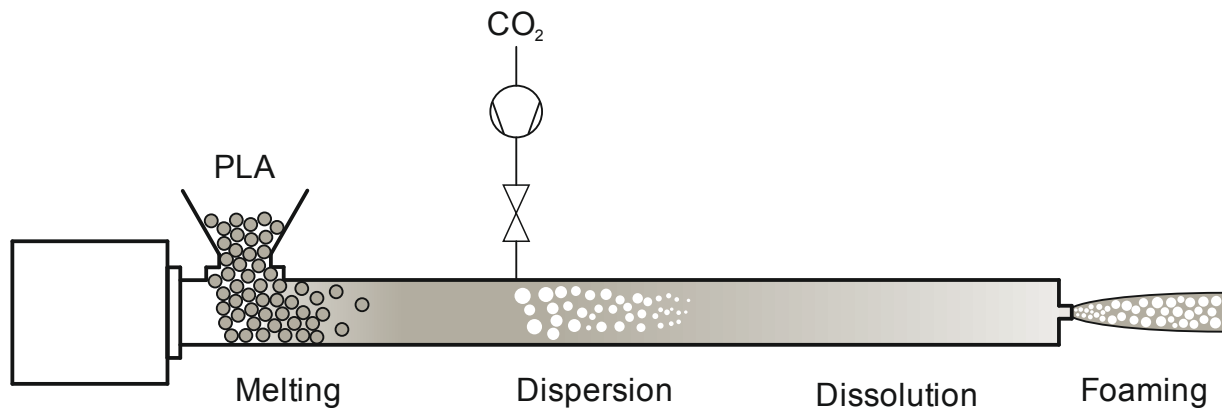


Fig. 2: Foam extrusion mechanisms

One approach to model gas dispersion in mixing devices is to investigate the forces affecting the fluid. Based on the arising strain rates and the stretching of fluid elements, statements on the bubble deformation and break-up can be made [3]. For this purpose, it is planned to use the CFD code ANSYS Fluent.

Summary

In this work, foaming the biopolymer PLA using CO₂ as blowing agent is investigated. Therefore, a discontinuous process as well as a continuous foaming process is investigated. Further steps are the implementation of the geometries and the material data into the CFD code to gain a deeper understanding of gas dispersion and dissolution phenomena in high viscous polymer melts that are relevant for foaming applications.

Acknowledgment

The discontinuous foaming experiments were performed by Blaž Haberman in the framework of his master thesis at the Institute of Thermo and Fluid Dynamics at the Ruhr-University Bochum.

References

- [1] K. Parker, J.-P. Garancher, S. Shah, A. Fernyhough, Expanded polylactic acid - an eco-friendly alternative to polystyrene foam, *Journal of Cellular Plastics* 47 (2011) 233–243.
- [2] M. Nofar, C.B. Park, Poly (lactic acid) foaming, *Progress in Polymer Science* 39 (2014) 1721–1741.
- [3] T. Lang, Dispergieren von Gasen in hochviskosen Flüssigkeiten mit SMX-Mischern, Dissertation, Shaker (2011).

Downstream Processing of Liquid Effluents of Biomass Hydrothermal Processing Plants

Marta Ramos Andrés

Department of Chemical Engineering and Environmental Technology, University of Valladolid, martaxra2@gmail.com

Introduction

The industry based on fossil raw materials will not be sustainable for many decades, and it is necessary to start the shift towards natural materials as the main source of carbon-based compounds. Following this strategy, the use of renewable resources contributes to climate change mitigation and environmental protection. The biorefinery approach centralizes biomass as the material to produce fuels, energy, heat and value-added chemicals. In a biorefinery, several processes of pretreatment, fractionation, conversion, and purification are combined to maximize the efficiency of the raw material in a sustainable manner.

The raw material of a biorefinery is the biomass. Lignocellulosic biomass is generally viewed as one of the sustainable sources since it is renewable, abundant, and distributed widely in nature. Biomass is primarily made up of three main types of biopolymers: cellulose (45-55%), hemicelluloses (25-35%), and lignin (20-30%) [1]. Regarding these biopolymers, hemicelluloses comprise a wide variety of monosaccharides including xylose, arabinose, glucose, galactose, mannose, fucose, gluconic acid, and galacturonic acid, depending upon the source [2].

Hemicelluloses, when are isolated from biomass, have a very broad variety of applications. They can be easily hydrolyzed into pentose (xylose and arabinose) and hexose (glucose, galactose, and mannose), and can be converted into fuel ethanol and other value-added chemicals, such as 5-hydroxymethylfurfural (HMF), furfural, levulinic acid, and xylitol. In addition, hemicelluloses can be converted into various biopolymers by modification, used as viscosity modifiers in food packaging film, as wet strength additives in papermaking, and as tablet binders [2].

In order to enable use of hemicelluloses, they must first be extracted from the biomass and then separated from the resulting solution by chemical and/or mechanical methods. The extraction methods include alkaline treatment, organic solvent treatment, mechanical-chemical treatments (ultrasonication, twin-screw extruder) and hydrothermal treatments [2]. The method used in this work was the hydrothermal one employing high

pressure and temperature water but below the critical point, to hydrolyze biomass for the continuous obtaining of hemicellulose and other bioproducts or biopolymers. During the hydrothermal process, the extracted acetyl groups from hemicelluloses autocatalyze the degradation of hemicelluloses to shorter chains, and consequently, the molecular weight of the polymer is decreased. The control of temperature and pH is a key factor in this process.

The composition of the solution after hemicellulose extraction depends on the raw material and the method, but in general, this solution is a complex mixture of the product (arabinoxylan) and impurities consisting of co-extracted molecules. These impurities must be removed before the use of the product. However, separation processes are often difficult because of the large number of substances present [3].

The most common methods used for the purification of hemicelluloses extracted are precipitation with ethanol, ultrafiltration, and chromatography. More homogeneous fractions are obtained by ethanol precipitation and chromatography, but low chemical consumption, low energy requirement, compactness and flexibility in equipment design, making it a highly attractive technology for laboratory and industrial scale [4].

The method used in this work to purify the extracted hemicelluloses was ultrafiltration. In the separation, the impurities should be removed with the ultrafiltration permeate, and the hemicelluloses should be concentrated in the retentate. When this concentration process is carried out directly after extraction, low initial flux and considerable flux decline with increasing hemicellulose concentration could be expected [3]. For this reason, the flux during the concentration of the hemicelluloses was prefiltered prior to ultrafiltration. The prefiltration method chosen was dead-end filtration due to its positive effect on ultrafiltration flux and the low product loss.

Ultrafiltration leads to increase concentration and it allows to separate the hemicelluloses depending on the molecular weight and the degree of polymerization. This degree of separation is essential for a future hydrolysis or spray dry.

Experimental

In this work, a previous extraction of hemicelluloses from lignocellulosic biomass was developed. Now the objective is the subsequent purification of the hemicelluloses. The biomass used is wheat bran and wood chips of *Catalpa bignonioides*.

The extraction is carried out in a continuous multistage pilot plant for biomass hydrolysis with subcritical water. It is constituted by 5 independent reactors that could be used individually or combined as the same system. Each reactor has a volume of 1 L. The maximum operational pressure and temperature are 20 bar and 180°C, although operational conditions have to be selected according to the biomass characteristics and the final desired product. This pilot plant can operate with a subcritical water flow rate up to 30 L/h.

Regarding the purification system, the main components are three tanks (feed, retentate and permeate containers), a peristaltic pump, a dead-end filter and a membrane module.

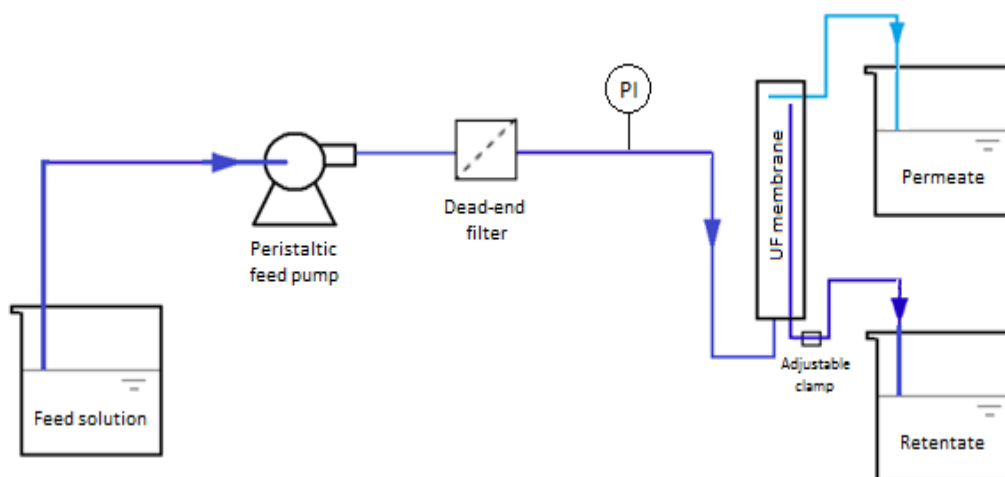


Fig. 1: Schematic flow diagram of the experimental system

Three cross-flow polyethersulfone Biomax™ ultrafiltration membranes are used, provided by Millipore Corporation (Bedford, MA) with nominal molecular weight cut-offs of 30, 10 and 5 kDa. The membranes were provided in plate-and-frame style Pellicon™ XL cassettes having a nominal membrane area of 50 cm².

The hemicellulose solution obtained from the hydrothermal extraction process is prefiltered by dead-end filtration before the membrane module with a 10 µm pore-size filter. Then the solution passes through the first membrane (30 kDa) and retentate is recirculated until a feed volume reduction of 80% is achieved. After that, the permeate solution passes through the following membranes (10 and 5 kDa) and retentate is also recirculated.

The transmembrane pressure is set in the range 1-1.5 bar and it is controlled by a manually adjusted clamp on the retentate side of the membrane. This transmembrane pressure is measured with a manometer at the inlet side of the membrane.

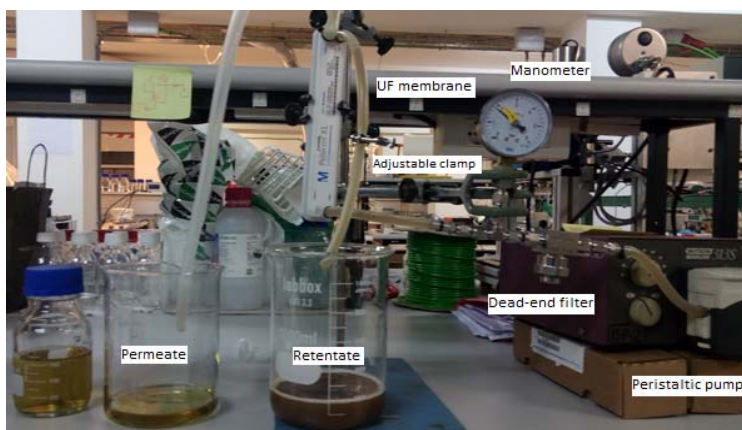


Fig. 2: Picture of the experimental setup

Summary

This thesis is targeted at the developing biorefinery processes using residual biomass. During the following years, it will be studied the fractionation of lignocellulosic biomass together with a subsequent hydrogenation of hemicelluloses. The technology used until now has been ultrafiltration of solutions from a hydrothermal extraction to purify the hemicelluloses before hydrogenation, drying or production of products such as aerogels.

Acknowledgment

This research has been financed by the Spanish Ministry of Economy and Competitiveness through the project CTQ2015-64892-R, "BIOFRAHYNERY".

MSc. Marta Ramos wish to acknowledge the Spanish Economy and Competitiveness Ministry for the scholarship/predoctoral contract.

References

- [1] P. Peng and D. She, "Isolation, structural characterization, and potential applications of hemicelluloses from bamboo: A review," *Carbohydr. Polym.*, vol. 112, pp. 701–720, 2014.
- [2] F. Peng, P. Peng, F. Xu, and R. C. Sun, "Fractional purification and bioconversion of hemicelluloses," *Biotechnol. Adv.*, vol. 30, no. 4, pp. 879–903, 2012.
- [3] H. Krawczyk, A. Arkell, and A. S. Jönsson, "Impact of prefiltration on membrane performance during isolation of hemicelluloses extracted from wheat bran," *Sep. Purif. Technol.*, vol. 116, pp. 192–198, 2013.
- [4] A. Arkell, H. Krawczyk, and A.-S. Jönsson, "Influence of heat pretreatment on ultrafiltration of a solution containing hemicelluloses extracted from wheat bran," *Sep. Purif. Technol.*, vol. 119, pp. 46–50, 2013.

Application of Fast Measurement Techniques to Safety Assessments of the High-Pressure LDPE Process: Decomposition and Pressure Release

Ömer Faruk Delibalta, TU-Darmstadt

Introduction

Pressure Relief systems are used to protect pressure vessels and related equipment against situations of excess pressure. In an emergency situation, they should vent sufficient mass to reduce the pressure to safety level. During the design of a High pressure LDPE Autoclave process an ethylene decomposition relief device sizing method was developed by DuPont in 1954. This design was based strictly on the operating conditions expected while making polymer. It did not consider start-up or shut-down conditions that could result in different requirements for the relief protection system. Neither position of the "Hot Spot" nor geometry effects were not included in DuPont sizing model. By using of fast measurement techniques decomposition relief phenomena in high pressure separators are characterized at different reaction conditions and described by applying of a thermodynamic model.

Experimental

The construction of the equipment is shown in Fig 1. Ethylene is taken from cylinders and compressed by means of a membrane compressor into storage vessels and the main autoclave which is designed for pressures up to 400 MPa. It has an inside diameter of 50 mm and a volume of 200 mL. The relief valve is a "normal closed" piston valve operated with PLC set pressure. To measure the flame front propagation as well as the pressure relief high sensitive piezoelectric sensors and custom made double Typ-S-thermocouples with high response characteristic are implemented in the reactor.

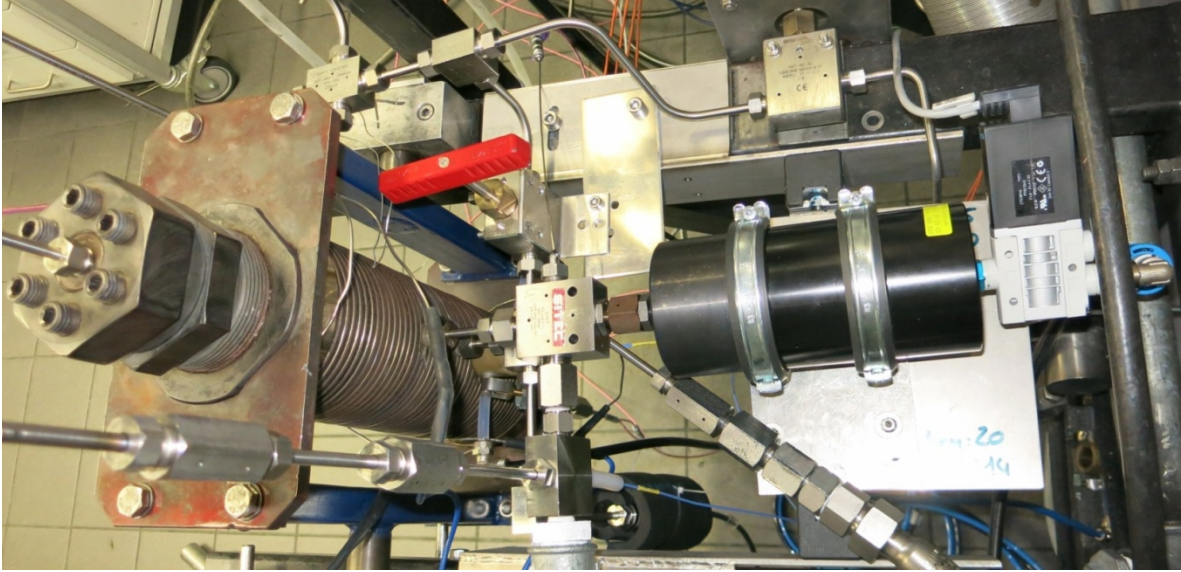


Fig 1: measurement device for decomposition relief experiments

For description of time pressure trajectories by venting of pure ethylene a one phase flow isentropic nozzle model is utilized. The maximal mass flow through the nozzle is calculated with LKP- and PC-SAFT equation of state at supercritical conditions and is applied for determination of the pressure and temperature trajectories by isentropic relief process. The discharge coefficient includes the geometry effects, also friction and heat transfer effects in the adiabatic nozzle, so it is also the ratio of mass flow in a valve to that in an ideal nozzle.

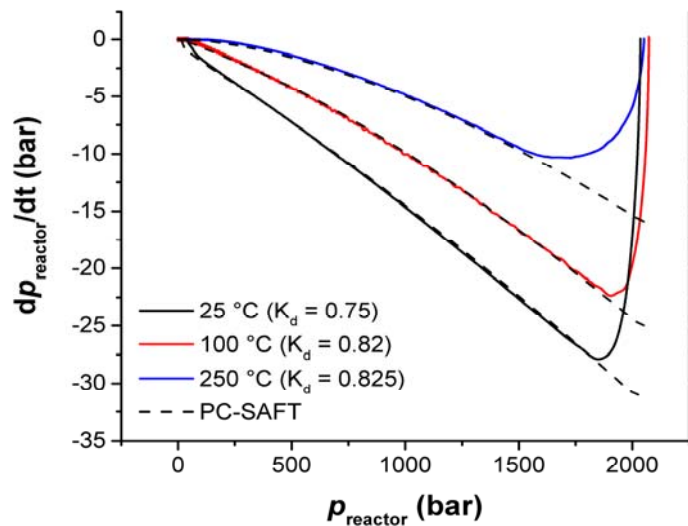
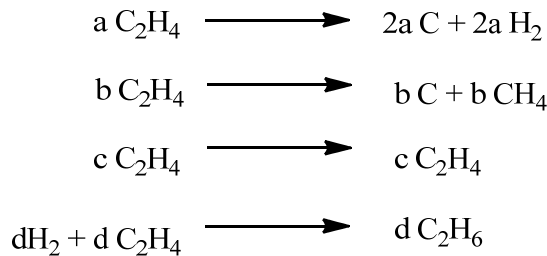


Fig 2: Discharge coefficient K_d for different T_0 by $p_0 = 2000$ bar and valve cross-section of 1mm

The pressure relief experiments are carried out by venting of nitrogen to analyse the dependence of different components. As result equivalent discharge coefficients are calculated.

To describe the decomposition of ethylene a thermodynamic model is developed by using of an adiabatic flame temperature. The kinetic of the reaction is implemented in the laminar burning velocity. A compartmentalization in burned and unburned volume during flame front propagation allows the calculation of the burned mass per time step, which is appropriate for the time pressure trajectories. For characterization of temperature gradients during slow decomposition of ethylene a heat transfer model is implemented in to the calculations. The radical decomposition steps are shown in next reaction equations.



The experimental burning velocities, determined by the thermocouples through the response time and measure point distance, for ignition at the top with a heat wolfram wire of the reactor at starting conditions of $T_0 = 250^\circ\text{C}$ and $p_0 = 300$ bar are compared with the calculated burning velocities in the next figure.

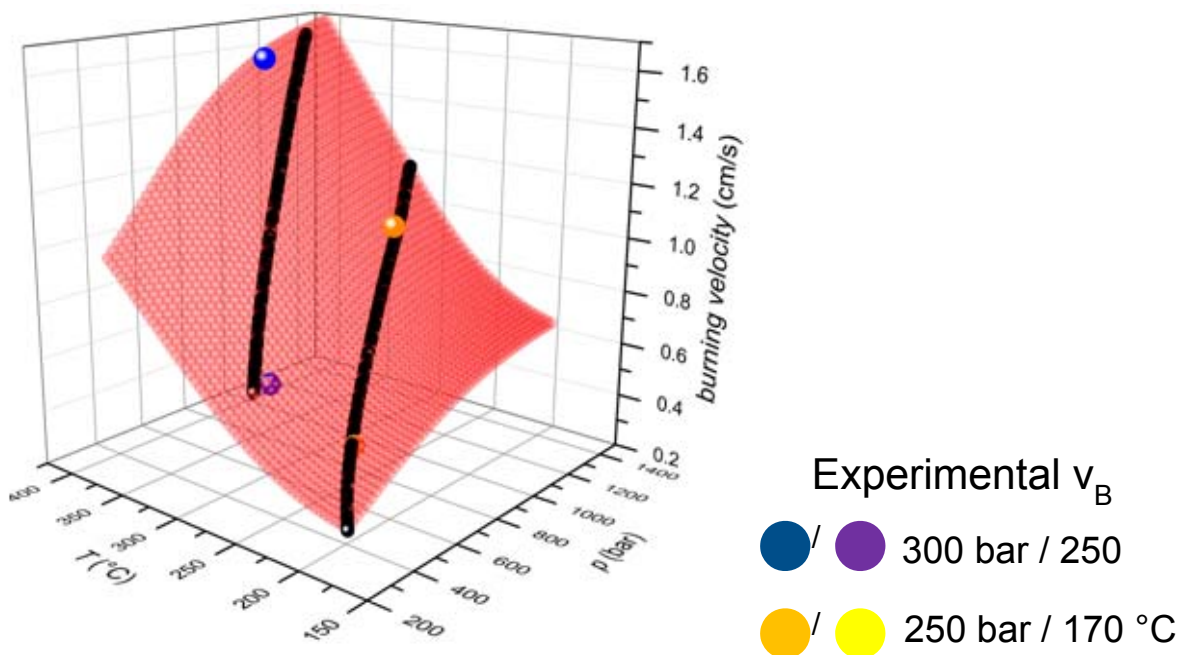


Fig 3: Calculated and measured burning velocity, starting conditions: $T_0 = 250^\circ\text{C}$ and $p_0 = 300$ bar

By implementation of a approximation function into the thermodynamic model for describing the burning velocity in depending of temperature and pressure conditions it is able to calculate the pressure trajectories of decomposition relief experiments. Resulting temperature and pressure profiles of a decomposition relief process are figured hereafter.

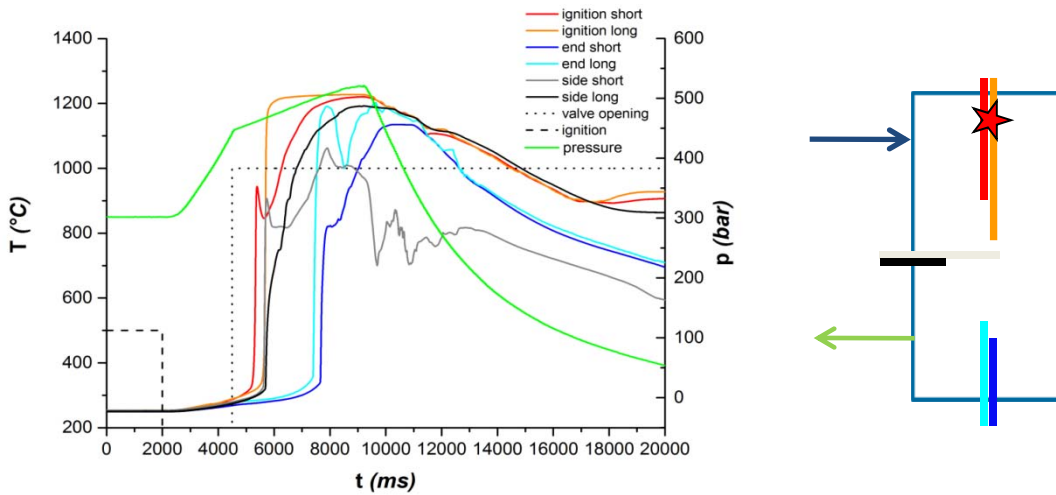


Fig 4: Decomposition and relief after ignition at the top of the reactor, $T_0 = 250^\circ\text{C}$ / $p_0 = 300$ bar

If the response characteristic of the thermocouples is analysed, a slow permanent flame front propagation with curved surface is observed in direction to the bottom of the reactor. After valve opening the pressure rise decreases up to a maximum and drops to atmospheric conditions. The waste gas temperature, measured by a Typ-N-thermocouple, concludes a relief of unburned gases up to the pressure maximum. After completion of the decomposition the pressure relief continues by venting of burned products.

Through combination of the adiabatic nozzle flow model and burning velocity model decomposition relief experiments could figured by applying of defined discharge coefficient, experimental adiabatic flame temperature and an enhancement factor for including of buoyancy effects during ethylene decomposition.

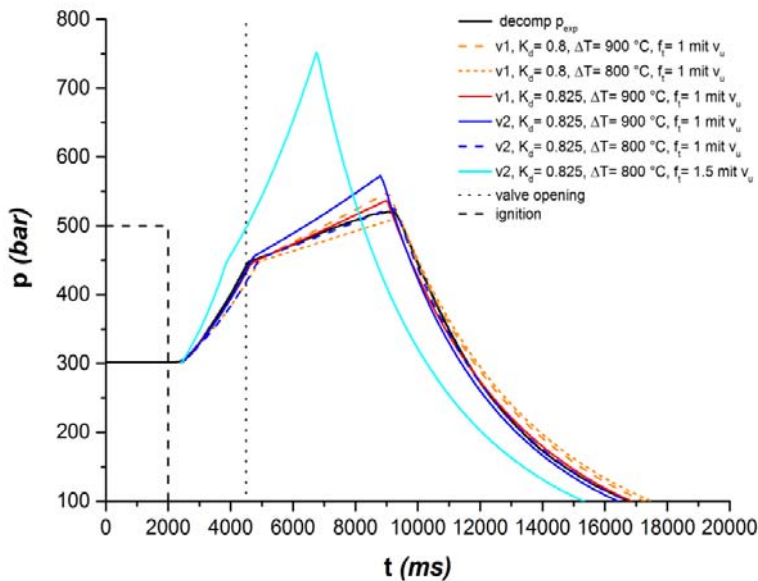


Fig 5: Simulation of pressure profile for ignition at the top of the reactor, $T_0=250^\circ\text{C}$ / $p_0=300\text{ bar}$

Summary

Defiance activation of the piston valve at defined set pressure the reactor pressure increases permanently because of high reaction rate of the decomposition process, so it is necessary to size the valve cross-section for reducing the pressure to safety level. Application of fast measurement techniques allows the analysis of the flame front propagation during decomposition event of ethylene. Calculation of the burning velocity as well as pressure relief process by a thermodynamic model enables a description of the transient pressure trajectories including discharge coefficient for characterization of none idealities in the piston valve and also different reactor conditions.

References

- [1] J. Albert, G. Luft, Thermal Decomposition of Ethylene-Comonomer Mixtures under High Pressure, Institut für chemische Technologie, Darmstadt, AIChE Journal, Vol. 45, No. 10, 1999.
- [2] T. Scheele, Explosionsauswirkungen bei thermischen Selbstzündung von verdichtetem Ethylen, Dissertation, Technische Universität Darmstadt, 2005.
- [3] A. Beune, Analysis of high-pressure safety valves, Dissertation, Technische Universität Eindhoven, 2009.
- [4] F. Mayinger, Stand der thermohydraulischen Kenntnisse bei Druckentlastungsvorgängen, Chem. Ing.-Tech. 53, 1981, Nr. 6, 424-432.
- [5] J. Broedermann, Druckentlastung und Ausbreitung der Zersetzungsfront am Beispiel der Hochdruckpolymerisation von Ethen, Dissertation, Technische Universität Darmstadt, 2006.

Extraction of Oil and OPC from Grape Seeds Using Supercritical CO₂ and Liquid-Liquid-Extraction

Samuel Theißl, Thomas Gamse

Institute of Chemical Engineering and Environmental Technology

Graz University of Technology

samuel.theissl@student.tugraz.at

Introduction

During the process of wine production, large amounts of waste in form of grape seeds are produced. These grape seeds still contain components, which when extracted can be used in a variety of applications. The focus here lies on grape seed oil and OPC.

Grape seeds are traditionally sold to the oil extraction industry and more recently they are asked for by cosmetic and pharmaceutical sectors for their use as a source of antioxidants [1].

Traditionally grape seed oil is extracted through mechanical pressure or by an organic solvent. While extraction with an organic solvent gives better yield, it also requires solvent recovery, additionally the quality of the product is inferior [2], extraction through mechanical pressure provides better quality of the extracted oil, but a lower yield.

As an alternative the use of supercritical CO₂ is promising, because it can achieve comparable oil yield with respect to conventional organic solvent extraction with better product quality similar to that of mechanical pressing [2].

OPC is a component found in several plants, in grape seeds the contents are especially high. It is desirable, because of medicinal use, it is sold in the form of powder or pills and research shows, that it lowers blood pressure and has other positive effects on the body. To extract the OPC a liquid-liquid-extraction in a Soxhlet-column is conducted.

Experimental

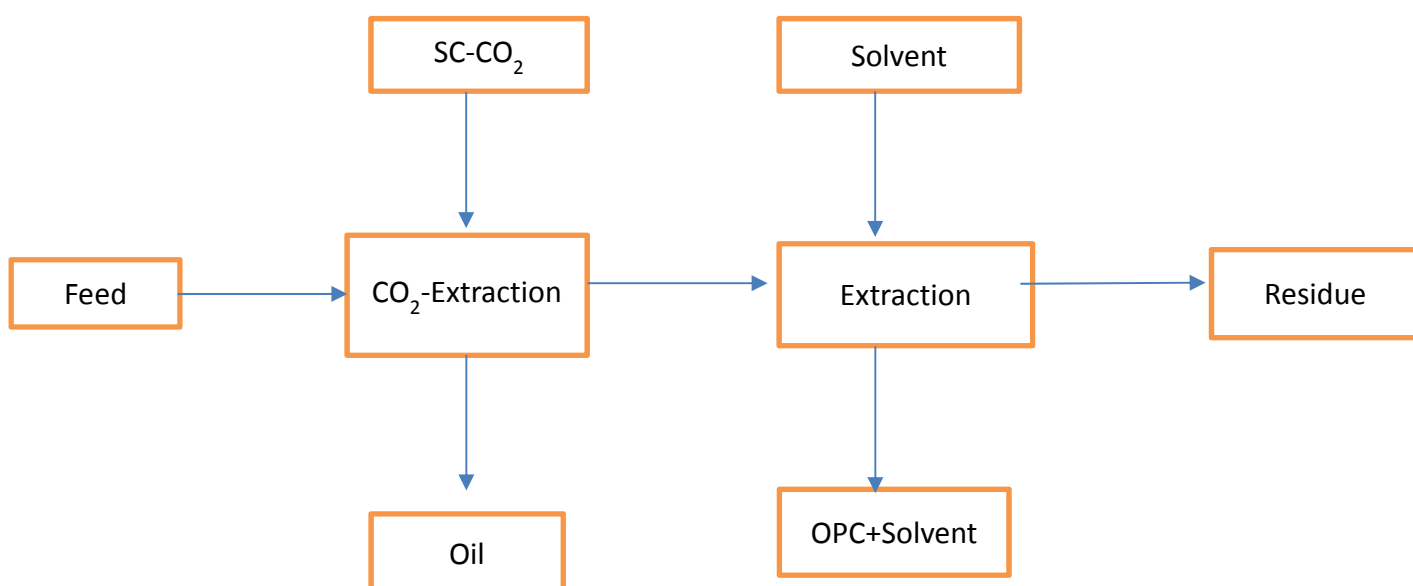
At the beginning the oil content of the grape seeds was determined at 12-14%, using a Soxhlet-column with Hexane as the solvent.

The extraction process is divided into two steps, the first one is to extract the oil with Supercritical CO₂, the second step is to extract the OPC using H₂O and Ethanol in a liquid-liquid-extraction.

When oil is extracted using mechanical pressing, 8-10% of the oil remains inside the residue, which then goes into the liquid-liquid-extraction.

During the extraction the SC-CO₂ flows through the grape seeds and extracts the oil compounds, which are separated in the down-stream process from CO₂. First tests have shown, that after using SC-CO₂ as extraction fluid the content of the oil in the residue is between 0,5-1%, depending on extraction parameters like flow-rate, pressure, temperature and extraction time.

The residue is subsequently treated in the Soxhlet-column for the liquid-liquid-extraction, using a mixture of H₂O and ethanol as solvent. The extraction takes place at constant temperature and standard pressure. The duration of the extraction takes several hours and the longer the extraction goes on the more OPC is extracted.



Pic.1: Flow-chart of the two stage extraction process

To analyse the extracts a HPLC method is used. The very small amounts of extracts are analysed under a specified light wave length range to obtain diagrams where the concentration of the wanted components can be determined.

Summary

Summarizing one can see that while the demand for both of these products is high, the methods to extract them can still be optimised. The main goal of these experiments is to find the best operating conditions, for a high yield, as well as to enable economic production.

References

- [1] L. Fiori, Grape seed oil supercritical extraction kinetic and solubility data: Critical approach and modelling, *The Journal of Supercritical Fluids* 43 (2007) 43-54

- [2] Kurabachew Simon Duba, Luca Fiori, Supercritical CO₂ extraction of grape seed oil: Effect of process parameters on the extraction kinetics, *The Journal of Supercritical Fluids* 98 (2015) 33-43

Foaming Virtualization and Characterization of Polymeric Foams

Robert Kuska

Thermo and Fluid Dynamics, Ruhr-University Bochum, Germany, kuska@vvp.rub.de

Introduction

This study aims at the virtualization of the foaming behavior of homogeneous physical foaming processes. An increased understanding of the bubble growth, bubble coalescence, flow behavior of porous materials and the main influences on the creation of the final foam products can be used for an optimization of an experimental process itself and for decreasing material waste. The *Volume of Fluid* method can be used to calculate the surface of the two-phase system [1]. A *User Defined Function* will be designed to manually control the pressure drop within the system by time. Considering a single bubble as well as multiple bubbles for the simulations lead to a visualization of the expansion ratio and interconnectivity of pores caused by a rapid pressure decrease. For the reason of validating the simulation with the real behavior, static foaming experiments are carried out. To set the process conditions, the thermal behavior at atmospheric and at elevated pressures of the biopolymer polylactic acid (PLA) as matrix material, and supercritical carbon dioxide (scCO₂) as blowing agent is investigated. The foams are characterized by the porosity and mean pore size considering various process parameters.

Experimental

In case of the experiments, an autoclave is used with a maximum pressure of 25 MPa, a maximum temperature of 200 °C and an overall volume of about 960 cm³ (see Fig. 1a). The untreated PLA pellets are filled inside a cylindrical mold with detachable bottom and perforated top to ensure a good contact between gas and pellets. After placing the mold inside of the autoclave, the autoclave is flushed with CO₂ before the temperature is increased to reach the chosen process conditions. Then, the CO₂ is filling up the autoclave and is compressed up to the chosen pressure. In the meantime, the CO₂ is dissolving into the PLA pellets. When the system temperature is higher than the melting temperature of PLA at the elevated pressure, the pellets melt together at the bottom of the mold. After the process temperature and pressure are achieved, the pressure is rapidly released, inducing a state of supersaturating the polymer phase with CO₂ and

resulting in bubble nucleation by physical foaming. A stable foam is achieved, once the temperature is reduced beneath the solidification temperature. The final foam state is created by further decreasing the temperature beneath the glass transition temperature of PLA.

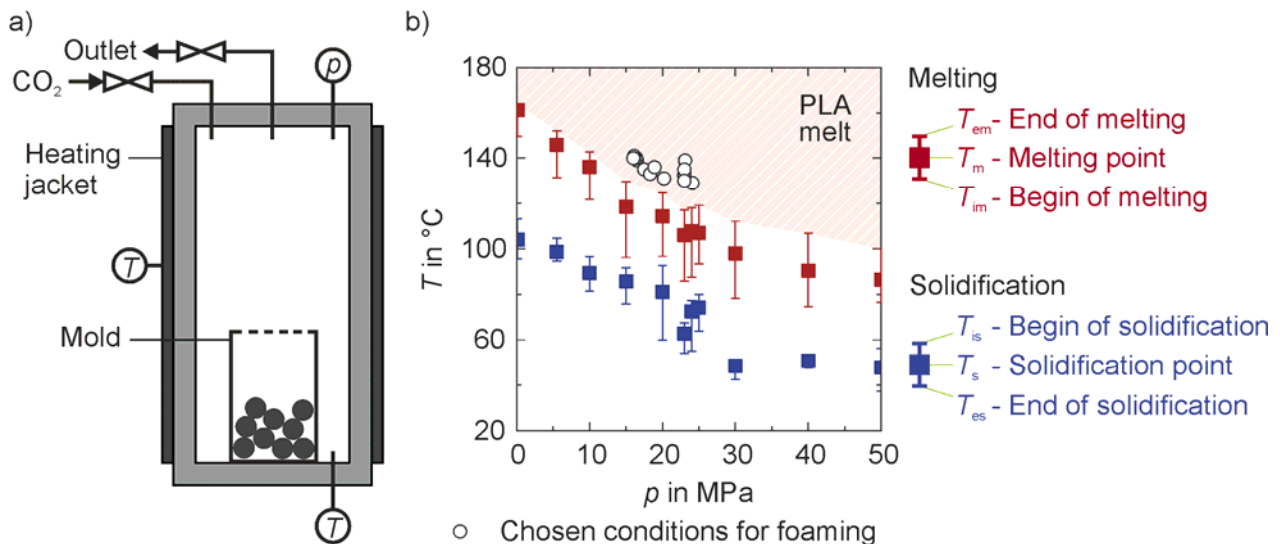


Fig. 1: a) Sketch of the cross section of the autoclave used for the foaming experiments ($V = 960 \text{ cm}^3$, $p_{\text{max}} = 25 \text{ MPa}$, $T_{\text{max}} = 200 \text{ °C}$) [2]. b) Measured melting and solidification (post melting crystallization) behavior by high pressure differential scanning calorimetry. The hatched area highlights the possible process area. The spheres visualize the chosen conditions for the foaming process [2].

The conditions chosen for the experiments are based on measurements by high pressure differential scanning calorimetry (HP-DSC) (see Fig. 1b). PLA is exposed to a CO₂ atmosphere with different pressures. The high CO₂ pressure not only leads to swelling of PLA by the dissolving of CO₂ [3], but also to a temperature depression of both, the melting and solidification behavior. This allows lower temperatures to achieve a PLA melt by using increased pressures in the system. Due to this, the process conditions are chosen close to the upper melting temperature T_{em} .

These experimental results are used for a validation of the simulation of the foaming process. The simulation has two goals: To achieve a better understanding of the foaming behavior itself within the matrix, the bubble interactions and coalescence are considered to visualize the foaming. First, the bubble nucleation needs to be realized as a starting condition for the simulation. In case of this study, a theory for homogeneous nucleation has to be used. Blander and Katz have set models for the calculation of the bubble nucleation already in 1975 [4]. The resulting nucleation rate is dependent on temperature and pressure. A rapid temperature increase or a rapid pressure decrease leads to a supersaturated matrix. If the gradient in the mentioned direction is great, the nucleation rate is large and a lot of bubbles nucleate.

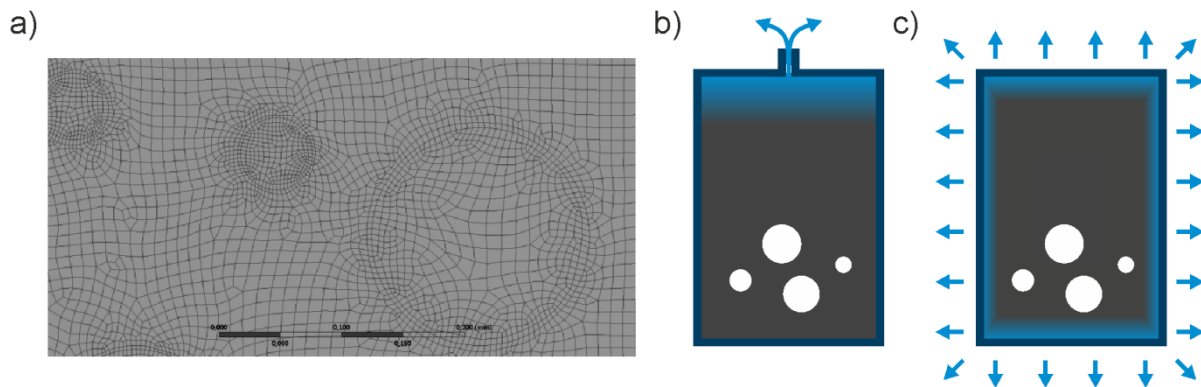


Fig. 2: a) Section of one of the used meshes at the surfaces of the gas bubbles [2]. b) Usual pressure release by a nozzle and pressure gradient within the area and c) a user defined pressure decrease at the boundaries of the area [2].

The transient simulation is realized in ANSYS Fluent. A two dimensional model is used with an area of 2 mm x 4 mm. Within this area, one or several bubbles are placed (see Fig. 2a). Besides using a laminar flow model, the numerical method used is the Volume of Fluid, as it describes a multiphase system and its surfaces. A static mesh is set which is more detailed at the phase interface between the gas and the matrix in the beginning of the simulation. While the matrix material is set to show constant properties, the density of the gas is calculated by the ideal gas law until a robust simulation is achieved. By this, a bubble growth caused by a density decrease is considered without any diffusion of CO₂ out of the matrix into the bubbles. Caused by these simplifications, especially the two dimensional observation, using a simple outlet with a pressure drop is not able to describe the real pressure decrease inside the system (see Fig. 2b). It is mainly used for the mesh independence test. Therefore, a user defined function (UDF) needs to be coded which exactly describes the pressure drop curve for the whole foaming time in the simulation. With this, different kinds of pressure release can be realized which may or may not have been used in experimental setups yet. To achieve a smooth pressure drop as in the case of a nozzle, the walls of the meshed area are manually changing the pressure with each time step (see Fig. 2c).

The aim of this work is the comparison of the simulated and visualized foaming with the experimental results. The afore mentioned simulation is the initial start. It still needs to be extended by further properties, as the viscosity and surface tension for both phases, namely CO₂ and PLA. In case of CO₂, an UDF based on an equation of state is necessary, too, since the ideal gas law does not consider any supercritical state. Furthermore, the diffusion of CO₂ out of the matrix into the nuclei is of high importance, as it is the main reason for the bubble growth. This is to be considered in a single bubble

simulation with implemented diffusion. Multiple bubble simulations are optimized to visualize the coalescence while expanding.

Summary

A visualization of a physical foaming process by an ANSYS Fluent simulation is planned. A manually implemented pressure regulation by a UDF is used to allow various pressure configuration curves for the simulations. After an initial and limited simulation is achieved, further properties are to be implemented to increase the grade of reality and to converge it more to the real behavior. This behavior is then to be compared with experimental data that were achieved in static processes within an autoclave.

References

- [1] C.A. Brebbia, P. Vorobieff, Computational Methods in Multiphase Flow VII, WIT Press, (2013).
- [2] R. Kuska, S. Frerich, Batch foaming of Poly(lactic acid) with supercritical Carbon Dioxide: Influences of process parameters on the morphology, Lisbon, Portugal, 16th European Meeting on Supercritical Fluids, 25.-28.04. (2017).
- [3] G. Li, H. Li, L.S. Turng, S. Gong, C. Zhang, Measurement of gas solubility and diffusivity in polylactide, Fluid Phase Equilibria 246 (1-2) (2006) 158–166.
- [4] M. Blander, J.L. Katz, Bubble nucleation in liquids, AIChE J. 21 (5) (1975) 833–848.

Numerical Investigations in a Novel Low-Shear Pressure Retention Valve for Hydraulic Applications

S. Ehsan Emamjomeh

Institute of Process Machinery and Systems Engineering,
University of Erlangen-Nuremberg, ehsan.emamjomeh@fau.de

Introduction

The aim of this project is to develop a retention valve for hydraulic applications which is adapted to the special properties and contents of hydraulic fluids. Additives in hydraulic fluids react very sensitively to shear and temperature and can be destroyed if shear forces and temperatures are too high, resulting in shortened service life of the fluid [1].

Our Institute with contribution of a Bavarian company has developed a novel control valve for thermal water circuits in recent years [2]. Emphasis was placed on a continuous control and a careful handling of the thermal-brine, since precipitation reactions, outgassing, cavitation and abrasive loss occur by severe turbulence fluid flows. This valve must be developed for further use in hydraulic applications. The differences compared to the use in thermal water are the partly significantly higher viscosities of the hydraulic fluids and the high pressures in hydraulic applications. Hydraulic oils have viscosities that are up to a factor of 500 times more than thermal water. The flow is therefore often laminar in contrast to turbulent water flow [1,3].

In the thermal water circuit, the valve is subjected to pressures of up to a maximum of 40 bar, whereas in the hydraulic pressures varies at 500bar and more. These high loads must be incorporated into the strength as well as the control concept. In comparison with conventional valves, the valve is intended to ensure a pressure control which is gentle regarding to the hydraulic fluid by the targeted prevention of shear loads. The reduction of shear loads and removal of the operational occurred dissipation heat are resulting an ultimately considerable extension of the service life of the hydraulic fluid [1,3].

This concept for pressure reduction consists of a cylindrical valve body which is placed into a precision pipe. The hydraulic oil flows along coil channel on the valve body in the pipe through a reduced cross-sectional area, where a pressure loss along the body is generated, which means that the pressure before the valve body increases. The sizing of the valve must be done in respect to the flowrate and pressure conditions of the different applications. The calculation algorithm applies equations of fluid mechanics to calculate the pressure drop in various pipe fittings. However, for this concept there is no

equation describing the pressure loss during tight cross-sectional area. Furthermore, few parameters and values for the equations had to be attributed empirically by means of experiments and simulations. Meanwhile, many different geometries were constructed on diverse scales to guaranty the general reliability of the calculation-tool [4].

Experimental

Figure 1 shows the computational fluid dynamics (CFD) simulation domain, which has been done to investigate the shear stress, pressure profile, and the flow velocity in pilot scale. For the following simulations, the software Star-CCM+ from Siemens/CD-adapco has been used. CFD program solves the Navier-Stokes equation numerically which explains the conservation of energy, mass, and momentum for the Newtonian fluids. The regime of the fluid in the valve is both turbulent & laminar and this can be solved with very high computational iterations. Thus, models were developed for a simplified description. Turbulent regimes are transient, but here for the simplification reasons the average values of the time-depending terms will be applied (Reynolds averaging) [4,5].

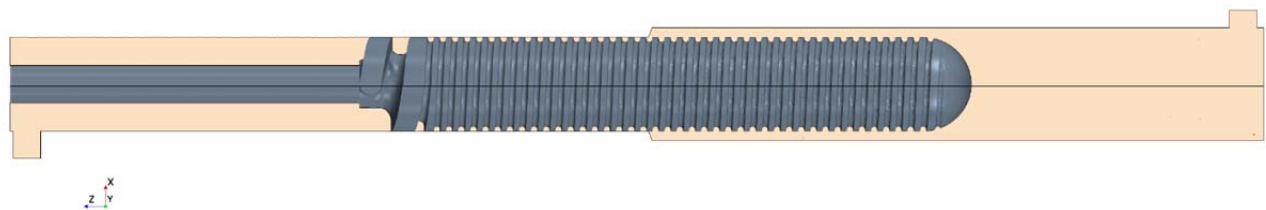


Fig. 1.: Simulation domain of the valve (valve position: half actuated)

Figure 2 shows that the maximum shear rate (red coloured parts) is reached only next to the edge of the groove (90° angle), where the fluid is forced out of the groove into the gap and only passes through a very narrow region of the precision pipe.

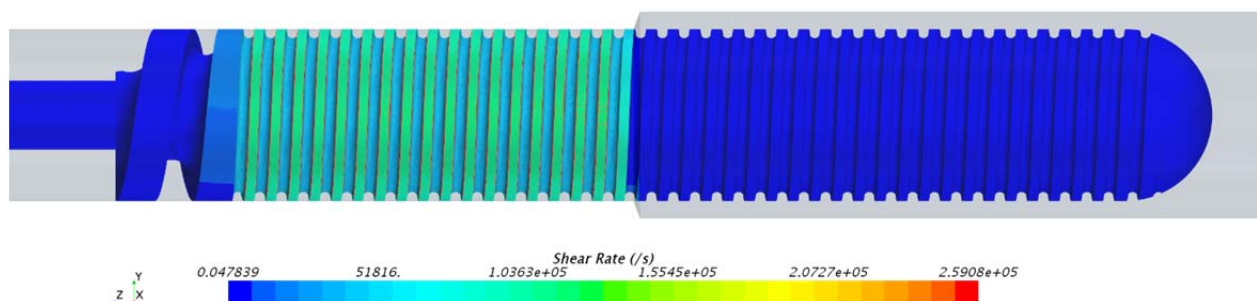


Fig. 2.: Shear rate at sharp edges of the valve for hydraulic oil (ISO VG 46)

Since the pressure difference between 2 grooves (left & right) and/or after one turn is relatively high, the fluid flow in the gap is inevitably accelerated. The gap size plays an

important role by shearing of the fluid, whereby two forces acting parallel to each other in opposite directions of two surfaces (outer of valve body and inner of precision pipe).

In the flow of a straight channel, the fluid does not move at the same velocity at each point of the channel. Instead, the fluid flow in the middle is the fastest and next to the wall is the slowest. This flow pattern is the result of friction within the fluid and between the fluid and the channel wall and refers to the fluid viscosity. This friction creates a tangential force exerted by the flowing fluid and is referred as the "wall shear stress".

Figure 3 represents the pressure loss profile inside the valve pipe, where the outlet-pressure of the hydraulic oil is set to 5 bar, an inlet-pressure of 281 bar is expecting.

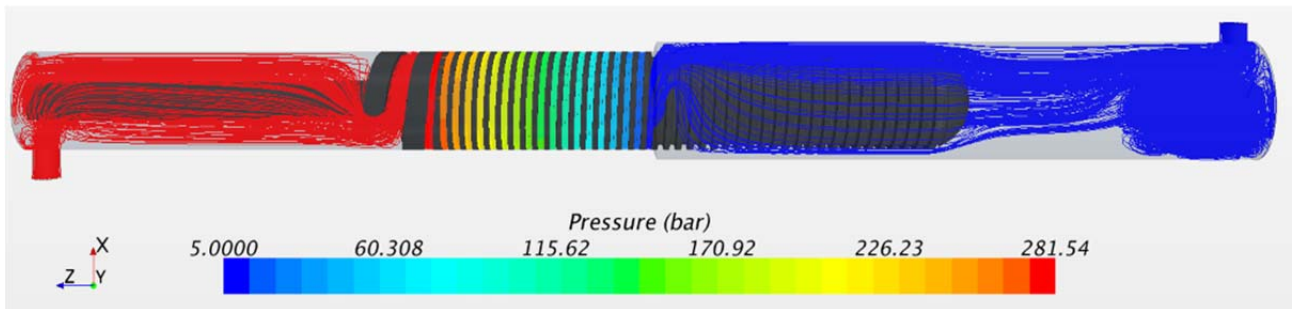


Fig. 3.: Total pressure by streamlines (valve position: half actuated)

Table 1 presents the results of 2 experiments for a fully actuated valve body within two different hydraulic oils systems. In both processes, the inlet average temperature was approx. 39°C and outlet approx. 46°C. The pressure reduction values for these tests are different and for the oil "B" this value is slightly higher.

Tab. 1.: Pressure reduction results from experimental tests at fully actuated position

No.	Oil	Avg. T_{out} (C)	Avg. T_{in} (C)	Position	P_{out} (bar)	P_{in} (bar)	ΔP (bar)
1	A	≈ 39°	≈ 46°	Fully actuated	3.1	300.2	297.1
2	B	≈ 39°	≈ 46°	Fully actuated	3.3	316.8	313.5

To perform a comparable simulation, the temperature profile along the valve tube and the respective viscosity and density values for each temperature is needed, so the fluid behaviour in the valve can be precisely described for CFD software. This is associated with a considerable number of sensor elements, time expenditure and a longer time for convergence. Therefore, for each experiment, 2 simulations are performed at the input/output temperature (see Table 2) and the arithmetical mean value of the pressure reduction is compared with experimental values. The physical properties at 39°C and 46°C were first measured, to be able to define the medium in the simulation software.

Tab. 2.: Pressure reduction results from experimentally comparable simulations

No.	Oil	T (C)	Position	P _{out} (bar)	P _{in} (bar)	ΔP (bar)	Avg. ΔP (bar)
1	A	39°	Fully actuated	5	343.8	338.8	301.65
2	A	46°	Fully actuated	5	269.5	264.5	
3	B	39°	Fully actuated	5	351.1	346.1	310.25
4	B	46°	Fully actuated	5	280.4	275.4	

For the oil "A", a mean value of 301.65 bar was reached, which compared to 297.1 bar, had a very good accuracy (error: 1.5%). The oil "B" with an average value of 310.25 bar against 313.5 bar also proved a very similar accuracy (error: 1%). Therefore, the reliability of the developed simulation model by us has been proven very successfully and this model can be used for further flow behaviour prediction in the valve.

Summary

Based on simulation results, when the gap size increases, the pressure drop and the shear rate decrease. For a higher pressure-reduction, the gap size must be kept as small as possible. Pipe thickness for the inlet and outlet sides of the valve may differ. Furthermore, a dependency of pressure loss and fluid viscosity has been observed.

Acknowledgment

The special thanks are to my colleagues Daniel Steger and Philipp Temme as well as our industrial partner for their cooperation on the practical experiments of this valve.

References

- [1] Peter Keith Brian Hodges: *Hydraulic fluids*. London and New York: Arnold; John Wiley & Sons, 1996. – ISBN 978–0–340–67652–3
- [2] A. Rauch, W. Zeilinger, P. Iberl, T. Weimann and E. Schlücker, *Drucksteuervorrichtung*. Germany Patent DE102014002845A1, 2014.
- [3] Watter, H.: *Hydraulik und Pneumatik: Grundlagen und Übungen - Anwendungen und Simulation; mit 23 Tabellen*. 2., überarb. Aufl. Wiesbaden: Vieweg + Teubner, 2008 – ISBN 978–3–8348–0539–3
- [4] Peter Iberl: *New Material Findings and Pressure Retention Concepts for an Efficient and Procedurally Safe Use of Deep Geothermal Brine*. Aachen: Shaker Verlag GmbH, Germany, 2016. – ISBN 978–3–8440–4616–8
- [5] H. Oertel jr and E. Laurien: *Grundgleichungen und Modelle, in Numerische Strömungsmechanik*, Chapter 3, Springer Fachmedien Wiesbaden, 2013, 143211.

Thermodynamic Studies of Adsorption on Porous Solids by Supercritical Fluid Chromatography (SFC)

Sheila Ruiz Barbero

Institute of Thermal Separation Processes, Hamburg University of Technology,
Germany. E-mail: sheila.ruiz@tuhh.de

Introduction

Silica aerogel particles have been shown to be a potential candidate for oral drug delivery system (DDS), where the loading of the drug is usually performed by adsorption from scCO_2 . Interactions between the drug and the matrix are crucial to the understanding of the loading mechanism. The use of silica aerogels as stationary phase in supercritical fluid chromatography (SFC) was studied in order to get a better understanding of the loading process and the interactions between the drug, the carrier and scCO_2 , and aerogel particles-packed column showed a good stability in an operation time of 48 hours in all the study cases [1,2]. As silica aerogel has a polar surface, polar compounds are more retained and the addition of a modifier (methanol) to the mobile phase is needed to be added in order to elute them. Due to this, retention in SFC is a complex function of the operating temperature, the pressure (or the density) of the mobile phase and its composition, as well as the properties of the solutes and the stationary phase. Many of these variables are interrelated and do not change in a predictable way [3]. Different Kromasil silica particles with different porous sizes were also analyzed and it was shown that the number of active sites, proportional to the surface area, have an influence on the retention time for polar compounds.

Experimental

The outcome of the liquid in supercritical fluid chromatography separation process is governed by the interactions between the solute and the mobile and stationary phase. The main characteristic property to study in SFC is the retention, which is described by the retention factor, k' . The retention factor is proportional to the distribution coefficient, and it expresses how much longer a sample component is retarded by the stationary phase than it would take to travel through the column with the velocity of the mobile phase. Mathematically, it is the ratio of the adjusted retention time and the hold-up time [4]:

$$k' = \frac{t_R - t_0}{t_0} = \frac{V_R - V_0}{V_0} \quad \text{Eq. (1)}$$

The hold-up time can be determined by the injection of nitrous oxide dissolved in methanol as unretained peak because it showed good results in all the studied columns and it was almost not affected by the concentration and the nature of the mobile phase [5]. The determination of the hold-up time is crucial because the retention factor will be introduced to two different models in order to extract useful information from the retention.

1. Linear Solvation Energy Relationships (LSERs)

First of all, the importance of various types of intermolecular interactions that reflect the properties of the stationary phases was evaluated by LSER regressions using 15 solutes. In this model, the retention was modelled as a function of a linear combination of five different terms, which represent five different kind of interactions (See Fig. 1). Capital letters represent the solute descriptors and they are universal constants, whereas lower letters represent the preferable interactions of a solute with the mobile or the stationary phase, and they are obtained by multilinear regressions at a certain temperature, pressure and concentration of modifier [6].

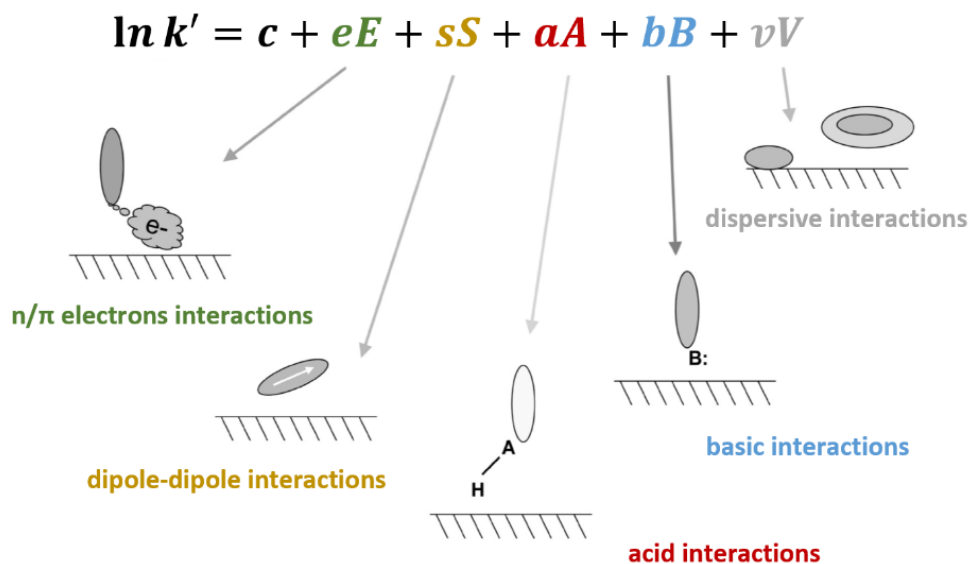


Fig. 1: LSER model and schematic representation of the different interactions [7]

Solutes can be classified into families according to the results of the LSER regressions, which were found that acid-basic interactions are the strongest one that affect retention in silica stationary phases. Each family of compounds showed a unique response to changes in concentration of modifier, temperature, and pressure, so that higher values increases, decreases, or has no effect on the retention factor.

2. Mixed Retention Model (MRM)

On the other hand, the addition of methanol as modifier has an influence on the properties of the mobile phase because it changes its density and polarity; but also on the stationary phase, because modifier molecules can deactivate adsorptive sites present on the surface of the packing material or the column wall. Furthermore, the adsorption of the modifier molecules can lead to swelling, which at the same time leads to an increase of the volume and an increase or decrease of the polarity of the stationary phase [3].

A Mixed Retention Model (MRM) was employed to take into account the effect of the modifier in the stationary phase. It considers that the retention depends on two types of interactions: apart from the contribution of the silanol groups, represented by k_0 , the adsorption of modifier on the surface of the stationary phase, represented by k_c , can also have an influence on the retention time (See Fig. 2). In such a way, k_0 represents the retention at zero percent concentration of modifier and it cannot be obtained experimentally. The influence of both contributions was described by the surface coverage fraction, θ , which represents the fractional occupancy of the modifier on adsorption sites (Eq. 2). The surface coverage fraction was approximated by the Langmuir adsorption model (Eq. 3) although it can be also obtained by Frontal Analysis (FA). The combination of Eq. 2 and Eq. 3 will lead to the adsorption isotherm model (Eq. 4) used to fitting the experimental data. K_{eq} was the equilibrium constant.

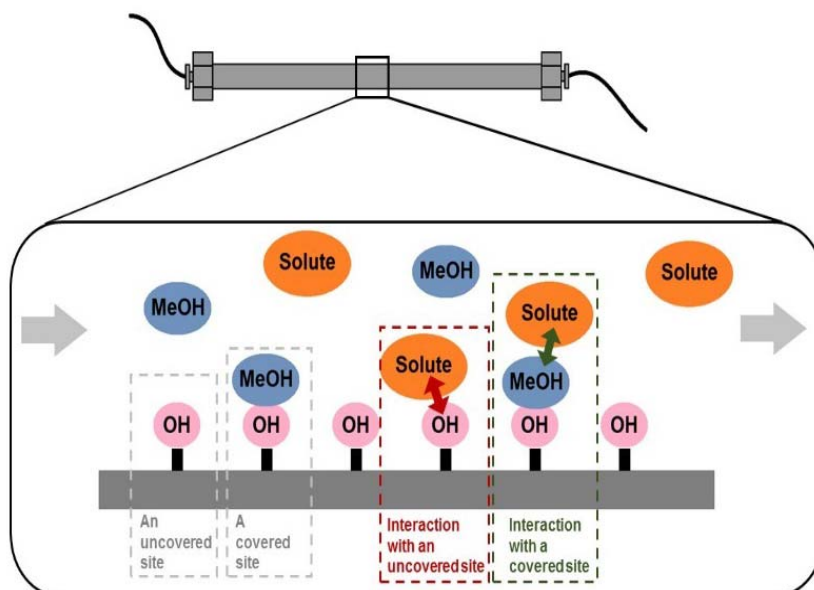


Fig. 2: Two types of interactions between the solute, modifier and stationary phase

$$k_{obs} = k_0(1 - \theta) + k_c\theta \quad \text{Eq. (2)}$$

$$\theta = \frac{N_s}{N_{max}} = \frac{K_{eq}x_{mod}}{1 + K_{eq}x_{mod}} \quad \text{Eq. (3)}$$

$$\longrightarrow k_{obs} = \frac{k_0 + k_c \cdot K_{eq} \cdot x_{mod}}{1 + K_{eq}x_{mod}} \quad \text{Eq. (4)}$$

The parameters k_0 and k_c were obtained from a curve in which the observed retention factor, k_{obs} , was plotted against the concentration of modifier, x_{mod} , at a certain temperature and pressure. The parameter k_0 was estimated at the intersection of the curve with the y-axis and it represents the contribution of uncovered sites to retention. The parameter k_c was obtained at a value in which the observed retention factor is not affected anymore by the concentration of the modifier. This is, the surface of the stationary phase is totally covered by the modifier. For further studies, the effect of the modifier in the mobile phase will be also considered.

References

- [1] Gurikov, P., Johannsen, M., & Smirnova, I. (2013). *Vestnik Sankt-Peterburgskogo University*, Serie 7: Geologia, G;2013, Issue 1, p278.
- [2] Guenther, U., Smirnova, I., & Neubert, R. H. H. (2008). *European Journal of Pharmaceutics and Biopharmaceutics*, 69(3), 935–942. <https://doi.org/10.1016/j.ejpb.2008.02.003>
- [3] Janssen, H. G., Schoenmakers, P. J., & Cramers, C. A. (1991). *Mikrochimica Acta*, 104(1–6), 337–351. <https://doi.org/10.1007/BF01245520>
- [4] Domínguez, J. G., & Diez-Masa, J. (2001). *Pure Applied Chemistry*, 73(6), 969–992.
- [5] Vajda, P., & Guiochon, G. (2013). *Journal of Chromatography A*, 1309, 96–100. <https://doi.org/10.1016/j.chroma.2013.07.114>
- [6] West, C., & Lesellier, E. (2007). *Journal of Chromatography A*, 1169(1–2), 205–219. <https://doi.org/10.1016/j.chroma.2007.09.011>
- [7] Lesellier, E. (2008). *Journal of Separation Science*, 31(8), 1238–1251. <https://doi.org/10.1002/jssc.200800057>

Characterization of Macromolecular Materials Under High Pressure

Nikolas Roß

Virtualisation of Process Technology, Ruhr University Bochum, ross@vvp.rub.de

Introduction

Macromolecular materials like polymers do accompany our daily life in numerous shapes such as packaging or isolation material. Even at high pressures, they are used as membranes, coatings or sealings. To gain new or specified material properties, polymers are processed in various procedures like foaming, extrusion or moulding.[2] Foamed polymers got very popular during the last centuries and has been widely investigated. By foaming polymers, less polymeric material is needed and specified product properties can be gained. While in former times volatile organic compounds like chlorofluorocarbons (CFC's) or hydrochlorofluorocarbons (HCFCs) were used as foaming agents, nowadays simple gaseous solvents like carbon dioxide (CO₂) become more common.[1] There are two phenomena occurring during processing polymers with a foaming agent like CO₂. First, CO₂ is absorbed into the polymer and due to that, the mass of the polymer phase increases. Simultaneously, the volume of the polymer sample increases and the polymer matrix changes.[1] The volume increase of the polymer is called swelling or dilation and depends on various process conditions like pressure, temperature and time of saturation. In addition, other parameters like aggregation of state or crystallinity of the polymeric material are influencing the product properties. In practical use, polymer swelling is relevant for the dimensional and chemical stability of polymeric sealings and for the stability of polymeric compound materials. Besides, another research motivation is the need of a correction factor for swelling simulations or foaming experiments.

The determination of swelling volume can be done based on several physical principles. Most common is the determination of the volume increase by visualization.[4] In general, a high pressure view cell with a sapphire window is equipped with a camera or a cathetometer to investigate the polymer swelling. Usually, the polymer height difference between the start and the end of the experiment is determined, and the swelling volume is calculated.

Other conventional methods use a spectroscopic method in combination with a high pressure cell or use electric measurements. In addition, there are several other approaches based on gravimetry and barometry or on oscillation or acoustic measurements.

Experimental

The aim of this work is to extend the knowledge of polymeric behaviour in presence of carbon dioxide. Hence, swelling and gas sorption in liquid and solid state will be investigated as well as diffusion coefficients and gas induced melting temperature decrease. Polymethyl Methacrylate (PMMA) is one of the most investigated polymers in this research area and will be analysed to validate the experimental setup. Additionally, Polylactic Acid (PLA), which is partially studied till now, will be further investigated. As solute material, CO₂ and nitrogen (N₂) will be used. CO₂ is a representative for the polar and nitrogen for the non-polar gases.

The experimental setup for the visual investigation of polymer swelling and the determination of solubility by the pressure decay method in this work mainly contains a high pressure view cell and a reservoir tank.

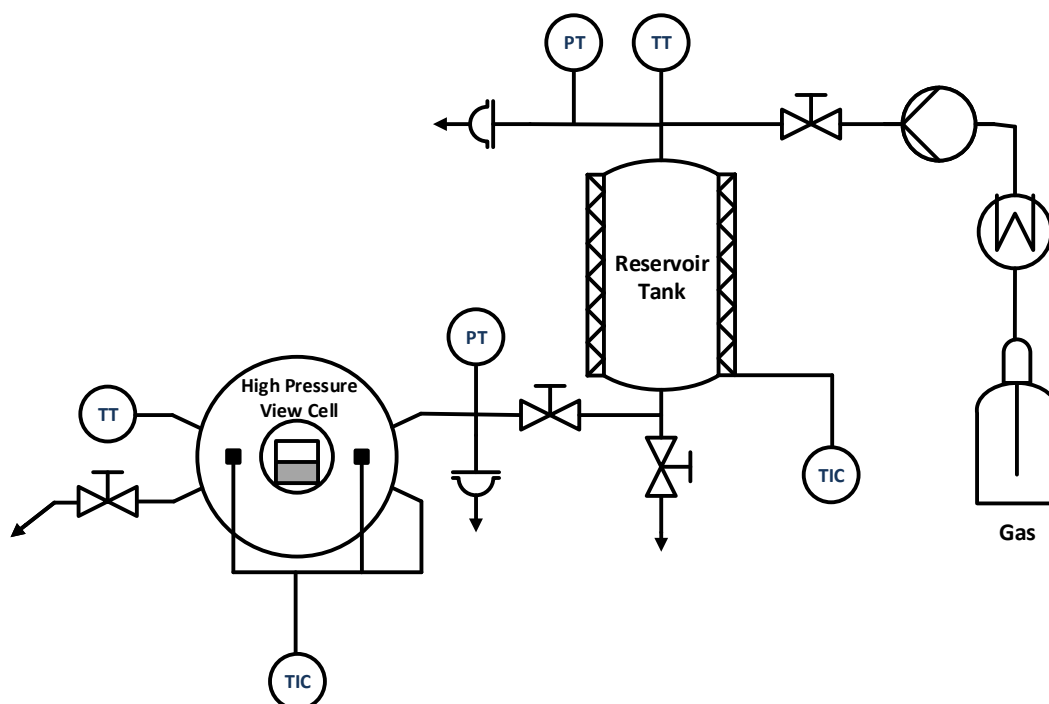


Figure 1.: Experimental setup for visual swelling investigations

The experimental procedure is divided into three steps. First, vacuum is drawn in the whole setup. Subsequently, the reservoir tank is filled with the investigated gas. Finally, the valve which separates the high pressure view cell and the reservoir tank is temporarily opened and the high pressure view cell is rapidly filled with gas. Due to sorption, a pressure drop in the high pressure view cell occurs. With the visual determined swelling volume and the pressure decay, the solubility of the gas in the polymer can be determined.

The thermal properties of polymers at elevated pressures is investigated by using a high pressure differential scanning calorimeter called "Transitiometer".

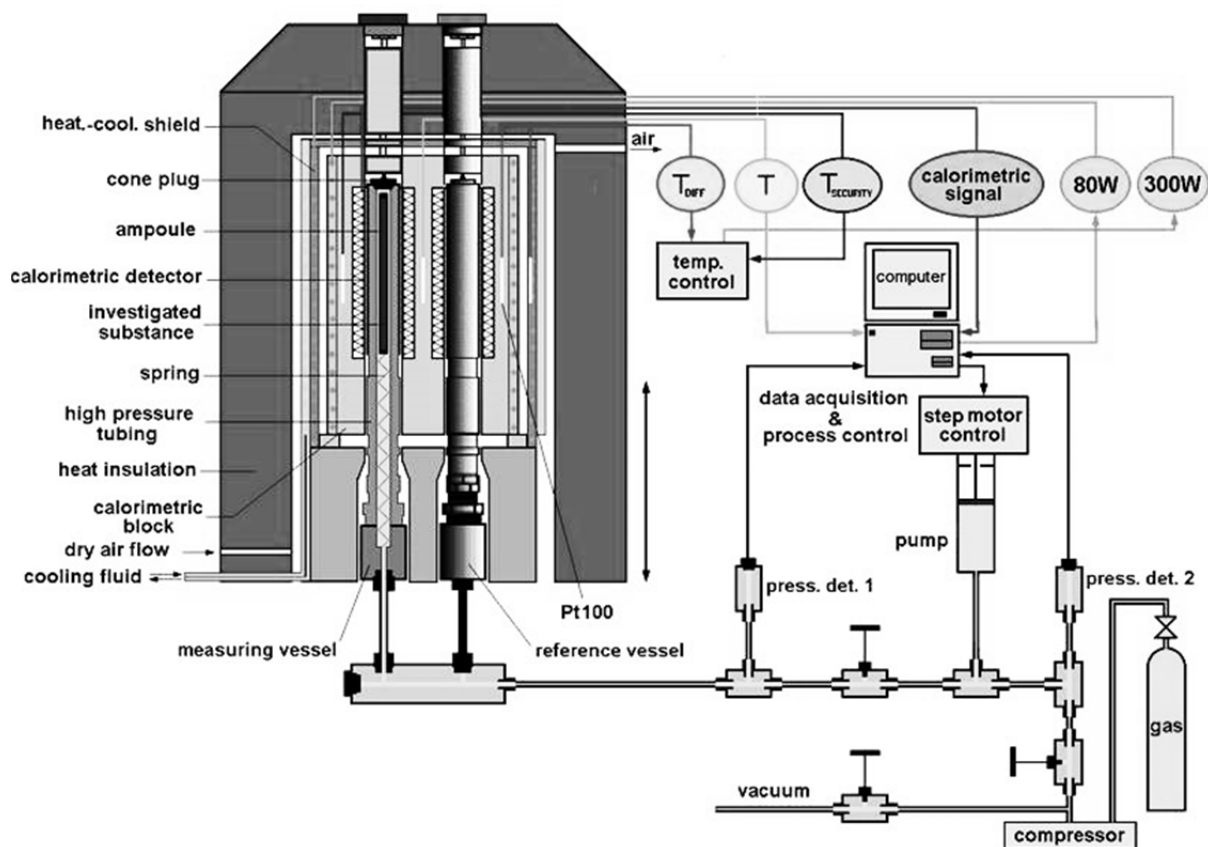


Fig. 2.: A schematic diagram of the current present Transitiometer setup [3]

The technical regulation will be realized with LabVIEW, after the renovation of some electro technical parts. Subsequently parameters like glass transition, melting and crystallinity temperature be determined.

Summary

Within the last decades many new ways to determine polymer swelling have been developed and known methods have been improved. These temporal evolution shows the importance of this research topic. With the high pressure view cell system and the Transitiometer an overall knowledge of polymeric behaviour under high pressures will be gained and present uncertainties like anisotropic swelling will be investigated.

References

1. Grolier J-PE, Randzio SL (2012) Simple gases to replace non-environmentally friendly polymer foaming agents. A thermodynamic investigation. *The Journal of Chemical Thermodynamics* 46:42–56. doi:10.1016/j.jct.2011.07.017
2. Nalawade SP, Picchioni F, Janssen L (2006) Supercritical carbon dioxide as a green solvent for processing polymer melts: Processing aspects and applications. *Progress in Polymer Science* 31(1):19–43. doi:10.1016/j.progpolymsci.2005.08.002
3. Randzio S, Stachowiak C, Grolier J.-. (2003) Transitiometric determination of the three-phase curve in asymmetric binary systems. *The Journal of Chemical Thermodynamics* 35(4):639–648. doi:10.1016/S0021-9614(02)00242-2
4. Wissinger RG, Paulaitis ME (1987) Swelling and sorption in polymer–CO₂ mixtures at elevated pressures. *J. Polym. Sci. B Polym. Phys.* 25(12):2497–2510. doi:10.1002/polb.1987.090251206

Parallelization of a Monte-Carlo Model for the Simulation of the Molecular Topology of LDPE

Oliver Salman, Markus Busch

Ernst-Berl-Institut für Technische und Makromolekulare Chemie,
Technische Universität Darmstadt, Oliver.Salman@pre.tu-darmstadt.de

Due to their wide range of applications, plastics are an important commodity in modern times. Referring to the entire production capacity of 58 million tons per year in Europe, about 17 % is constituted by LDPE (low-density polyethylene).^[1] LDPE is produced by free-radical polymerization under high-pressure conditions between 1500 bar and 3500 bar in autoclave or tubular reactors. Its properties are mainly determined by the molecular microstructure that is strongly influenced by the process conditions. Because of the free-radical nature of the ethane polymerization, low-density polyethylene consists of highly branched molecules. In order to describe the polymer structure of LDPE and to obtain predictions of the materials behavior, process simulations based on experimental data have got an important tool for process engineering.^[2,3]

Eric Neuhaus and *David Eckes* developed a hybrid approach combining a deterministic and a stochastic model for the LDPE process.^[4,5] To simulate the mass and heat balance, the deterministic approach is used to solve a system of partial differential equations based on the kinetics of the free radical polymerization. For this purpose the commercial program PREDICI[®] is used that is able to handle molecular distributions in a very efficient way. The detailed molecular microstructure itself is simulated by a stochastic Monte-Carlo model. This Monte-Carlo model creates a set of polymer molecules based on the conditions calculated in the deterministic model. Figure 1 shows the workflow of this hybrid approach.

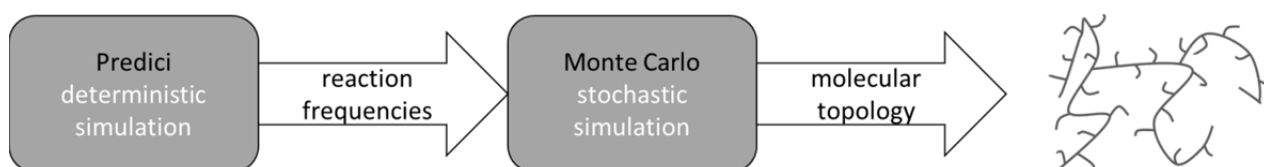


Figure 1: Principle of the hybrid deterministic and stochastic approach to simulate the molecular microstructure of LDPE.

In order to obtain statistically relevant results from the Monte-Carlo simulation, a sufficiently large ensemble of molecules must be simulated, which in turn takes a lot of computing time.

To reduce the simulation time, the Monte-Carlo algorithm, which is written in the programming language Fortran, is parallelized with the OpenMP standard for shared-memory programming. For this, the OpenMP standard includes compiler directives and library routines to create programs, which are running on multicore computers with shared memory.

The originally Monte-Carlo algorithm simulates the molecule ensemble serially in a loop, where each loop iteration creates a single molecule. By parallelization of this algorithm with OpenMP, the main loop that simulates the molecule ensemble is executed on several processors. This means, each molecule is calculated by one processor and several molecules are processed at the same time. Figure 2 shows the loop and compares the serial and the parallel execution of the Monte-Carlo program.

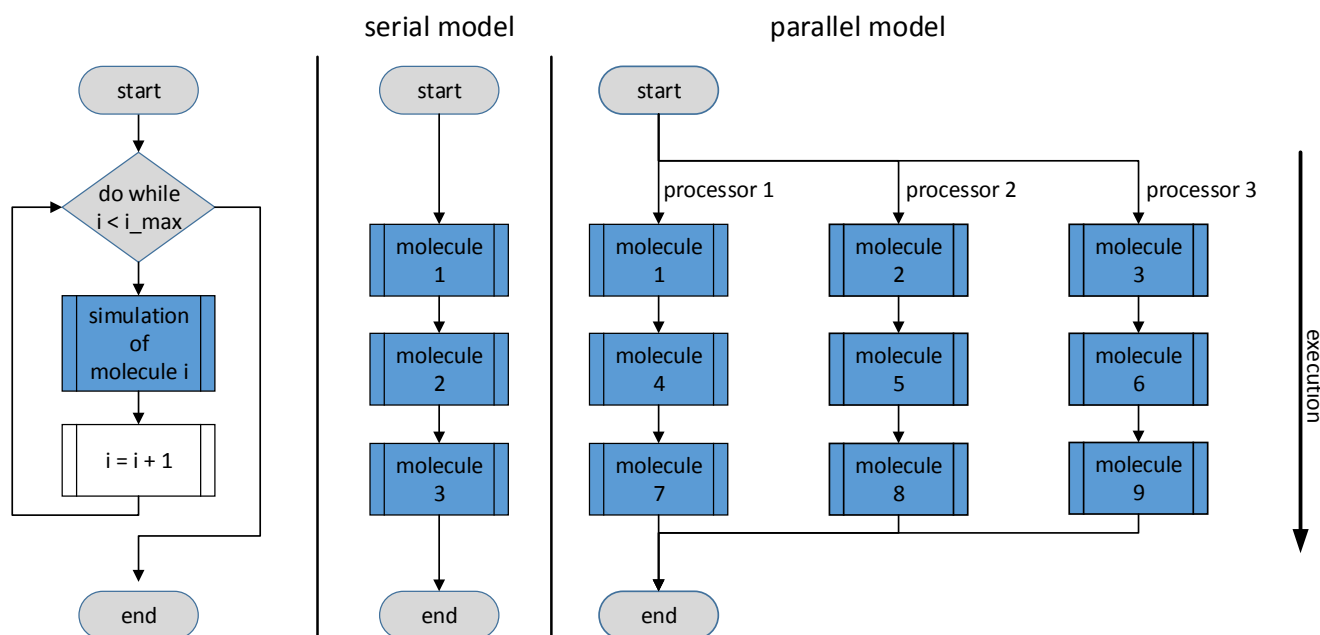


Figure 2: Parallelized loop of the Monte-Carlo algorithm to simulate an ensemble of LDPE molecules.

The reaction network of the free radical polymerization of ethene includes bimolecular reactions. Because of these bimolecular reactions, molecular information has to be

exchanged between the processors. Therefore, this information is stored in shared data addresses of the common memory. With parallel programming, additional challenges emerge. Serial programs process the individual instructions successively. On parallel computers, it can occur that instructions and data accesses happens simultaneously. To avoid unpredictable runtime errors, it is necessary to synchronize the accesses of shared data. For this synchronization, OpenMP provides a set of tools. Due to these synchronizations, it is not possible to get a linear speed up scalability of the Monte-Carlo Program.

However, by parallelization of the Monte-Carlo algorithm, a significant speed up is achieved. Compared to the serial execution, the parallel program on average is 4.1 times faster on a computer with eight logical cores. This means, a processor efficiency of more than 50 % was achieved.

References

- [1] PlasticsEurope, *Plastics - the Facts*, **2016**.
- [2] F. Ullmann, *Ullmann's Encyclopedia of Industrial Chemistry*, Wiley, Weinheim, **2000**.
- [3] G. Luft, *Chemie in unserer Zeit* 34, 190-199, **2000**.
- [4] E. Neuhaus, Dissertation: *Hybridsimulation der industriellen Hochdruckpolymerisation von Ethen*, TU Darmstadt, **2014**.
- [5] D. Eckes and M. Busch, *Macromolecular Symposia* 360, 23-31, **2016**.

Development of Novel Nozzle Geometries for Carbon Dioxide Jet Cutting Applications

Niklas Strauch

Chair of Process Technology, Ruhr-University Bochum, strauch@vtp.rub.de

Introduction

The use of high pressure water jets is well established in industry for cutting applications. To improve the cutting performance abrasive substances can be added to the water jet. However, residues of the abrasives may remain on the workpiece, and water-sensitive materials cannot be processed. Additionally, when cutting contaminated materials, an extensive cleaning step may be required in order to decontaminate the used water. These disadvantages lead to the motivation for finding an alternative cutting technology. The use of liquid carbon dioxide instead of water as the cutting medium allows residual free and dry processing. Engelmeier et al. [1] also showed that liquid CO₂ jets allow drilling more precise holes in comparison to water jets as shown in Fig. 1.

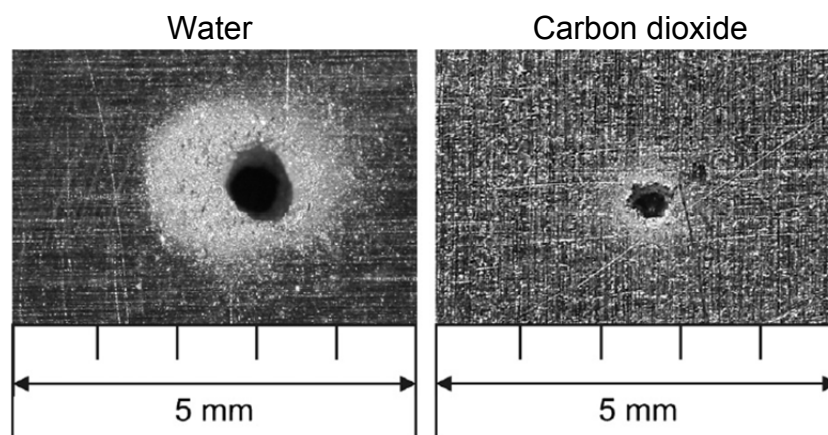


Fig. 1: Comparison of holes in aluminium drilled by a water and a carbon dioxide jet [1]

Therefore, the main objectives for future works are to generate further knowledge of the formation and stabilization of liquid CO₂ jets as well as their cutting properties. CO₂ is compressed to pressures of up to 400 MPa, set to the desired temperature, and rapidly expanded to atmospheric pressure through a nozzle. The jet is directed on sample materials of varying hardness.

Under atmospheric pressure and in thermodynamic equilibrium, CO₂ can only exist in gaseous or solid state. However, Engelmeier et al. [2] found a way to form liquid CO₂ jets at atmospheric pressure that can be used for cutting and drilling applications. The

key factors for the formation of those liquid CO₂ jets were found to be the pre-expansion pressure and temperature as well as the expansion through a sharp-edged nozzle.

Experimental

The setup of the plant is shown in Fig. 2. Liquid carbon dioxide is cooled and compressed in a high pressure pump to up to 3500 bar. It is then led through a heat exchanger in order to control the temperature prior to the expansion through a nozzle to atmospheric pressure. A particle image velocimetry (PIV) system, in which a laser is used as a light source, allows visual observation of the resulting jet. The laser, the high-speed camera, and the jet are arranged in an optical axis as indicated by the dashed lines in Fig. 2. The laser is equipped with a diffusor plate, which allows only the emission of light with a wavelength of 574-580 nm. The pulse duration is 20 ns. The camera is of the model imager sCMOS (LaVision) with a resolution of 2560×2160 pixel. This setup allows sharp imaging of the jet despite high jet velocities.

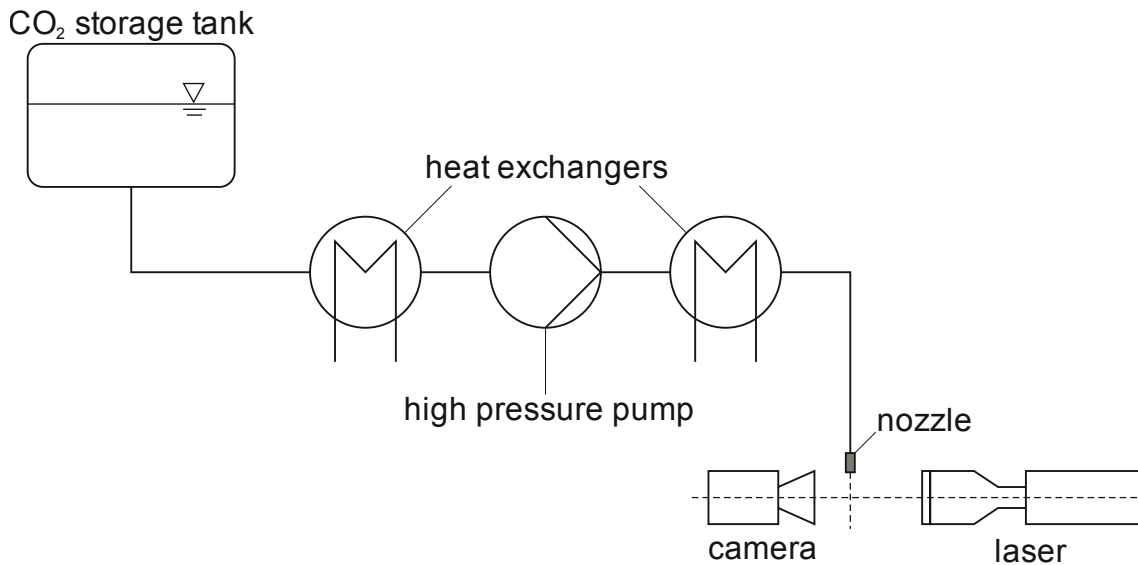


Fig. 2: Schematic experimental setup

Outlook

Future investigations will focus on effects inside the nozzle. Therefore, numeric simulations of the fluid mechanics happening in the nozzle will be conducted. The simulations will be validated by experiments carried out with the plant described above. In those validation experiments, a transparent nozzle will be used. Hence, effects before

and inside the nozzle can be observed through the PIV system. Based on the simulation's results different nozzle geometries will be designed.

Acknowledgement

The author would like to thank the Deutsche Forschungsgemeinschaft (DFG) for financial support.

References

- [1] Engelmeier, L., Pollak, S., Kilzer, A., Weidner, E. (2012), *Liquid carbon dioxide jets for cutting applications*, Journal of Supercritical Fluids (69), 29-33
- [2] Engelmeier, L., Pollak, S., Weidner, E. (2017), *Investigation of superheated liquid carbon dioxide jets for cutting applications*, Journal of Supercritical Fluids, in Press, available online since 27 January 2017

Registered Lecturers

Prof. Zeljko Knez	University of Maribor, Slovenia zeljko.knez@uni-mb.si
Prof. Urban Bren	University of Maribor, Slovenia urban.bren@um.si
Dr. Amra Perva-Uzunalic	University of Maribor, Slovenia amra.uzunalic@um.si
Dr. Masa Knez-Hrncic	University of Maribor, Slovenia masa.knez@um.si
Ao.Prof. Thomas Gamse	Graz University of Technology, Austria Thomas.Gamse@TUGraz.at
Dr. Eduard Lack	Natex Prozesstechnologie, Austria office@natex.at
Dr. Helena Sovova	Academy of Sciences of the Czech Republic, Czech Republic, sovova@icpf.cas.cz
Prof. Marcus Petermann	Ruhr University Bochum, Germany petermann@fvt.ruhr-uni-bochum.de
Prof. Markus Busch	Technical University Darmstadt, Germany markus.busch@pre.tu-darmstadt.de
Prof. Eberhard Schlücker	University Erlangen Nürnberg, Germany sl@ipat.uni-erlangen.de
Dr. Carsten Zetzl	Hamburg University of Technology, Germany zetzl@tuhh.de
Dr. Pavel Gurikov	Hamburg University of Technology, Germany pavel.gurikov@tuhh.de
Prof. Maria Jose Cocero	University of Valladolid, Spain mjcocero@iq.uva.es
Prof. Angel Martin Martinez	University of Valladolid, Spain mamaan@iq.uva.es
Prof. Esther Alonso Sánchez	University of Valladolid, Spain ealonso@iq.uva.es

Prof. Jacques Fages	Ecole des Mines d'Albi, France Jacques.Fages@mines-albi.fr
Prof. Edit Szekely	Budapest University of Technology and Economics, Hungary, sz-edit@mail.bme.hu
Dr. Alessandro Zambon	University of Padua, Italy zambon.alessandro@gmail.com
Prof. Ludo Kleintjens	DSM Company / Ruhr University Bochum, The Netherlands, ludo.kleintjens@hetnet.nl
Prof. Irena Zizovic	University of Belgrade, Serbia zizovic@tmf.bg.ac.rs
Prof. Carl Schaschke	Abertay University, United Kingdom c.schaschke@abertay.ac.uk

Registered Participants

Gregor Hostnik	SI	University of Maribor
Samuel Theißl	AT	Graz University of Technology
Diana Keddi	DE	Ruhr University Bochum
Margarethe Roskosz	DE	Ruhr University Bochum
Judith Janowski	DE	Ruhr University Bochum
Robert Kuska	DE	Ruhr University Bochum
Nikolas Roß	DE	Ruhr University Bochum
Niklas Strauch	DE	Ruhr University Bochum
Karen Fuchs	DE	Fraunhofer UMSICHT, Oberhausen
Daniel Steger	DE	Universität Erlangen-Nürnberg
Arian Shoshi	DE	Universität Erlangen-Nürnberg
Ehsan Emamjomeh	DE	Universität Erlangen-Nürnberg
Ömer Deliblata	DE	Technical University Darmstadt
Paul Peikert	DE	Technical University Darmstadt
Oliver Salman	DE	Technical University Darmstadt
Sheila Ruiz Barbero	DE	Hamburg University of Technology
Miaotian Sun	DE	Hamburg University of Technology
Marc Conrad	DE	Hamburg University of Technology
María Andérez Fernández	ES	University of Valladolid
Marta Ramos Andrés	ES	University of Valladolid
Tijana Adamovic	ES	University of Valladolid
Ana Sofia Martins Roda	PT	University of Oeiras

Book of Abstracts

ESS-HPT 2017 The European Summer School in High Pressure Technology

2.7.-16.7.2017, University of Maribor and Graz University of Technology

ISBN (e-book) 978-3-85125-541-6

DOI 10.3217/978-3-85125-541-6

Year of Publication: 2017